Phys. Lett. B 877 (2026) 140279

Contents lists available at ScienceDirect

Physics Letters B

journal homepage: www.elsevier.com/locate/physletb

Letter

Search for Higgs bosons produced in association with a high-energy photon via vector-boson fusion and decaying to a pair of b-quarks in the ATLAS detector

The ATLAS Collaboration [1]

ARTICLE INFO

Editor: Dr. M. Doser

Keywords:
Higgs boson
Vector boson fusion
Higgs plus photon production
Higgs decay to bottom quarks
ATLAS experiment
Large Hadron Collider

ABSTRACT

A search for Standard Model Higgs bosons produced in association with a high-energy photon and decaying to $b\bar{b}$ is performed using $133\,\text{fb}^{-1}$ of $\sqrt{s} = 13$ TeV pp collision data collected with the ATLAS detector at the Large Hadron Collider at CERN. The photon requirement reduces the multijet background, and the $H \to b\bar{b}$ decay is the dominant decay mode. Event selection requirements target events produced by vector-boson fusion, the dominant production mode in this channel. Several improvements enhance the search sensitivity compared to previous measurements. These improvements include better background modelling and characterization, the use of a neural-network classifier, and an updated signal extraction strategy adopting a direct binned-likelihood fit to the classifier output. With these improvements, the Higgs boson signal strength is measured to be 0.2 ± 0.7 relative to the Standard Model prediction. This corresponds to an observed significance of 0.3 standard deviations, compared to an expectation of 1.5 standard deviations assuming the Standard Model.

1. Introduction

The scalar Higgs boson, discovered in 2012 [1,2], has been studied extensively in all the expected main production modes and in many of its decay channels. The Higgs boson decays most frequently to a pair of b-quarks, making this a powerful decay channel to study. However, this decay is challenging because of a significant non-resonant QCD multijet background, which complicates the search. By requiring a final state with an associated high-energy photon, a destructive interference effect, arising from diagrams with initial-state and final-state radiation of the photon, reduces this non-resonant background, making this an interesting final-state signature to target [3]. An example Feynman diagram for this dominant non-resonant background is shown in Fig. 1a. Conveniently, the photon also provides a clean signature on which to trigger. Due to the increased number of electroweak vertices in vector-boson fusion (VBF) Higgs boson production, this production mode surpasses gluon–gluon fusion (ggH) and becomes the dominant production mechanism when an associated photon is required. The leading-order Feynman diagram for this mode is shown in Fig. 1b. By requiring a high dijet invariant mass, the signal phase space becomes purer in VBF Higgs production, with vector-boson associated Higgs production ($VH, V = W, Z$) contributing less than 5% of the signal. Additionally, a destructive interference effect, similar to that reducing the non-resonant QCD multijet background, suppresses ZZ-fusion and makes this a unique way to study WW-fusion Higgs production and the HWW interaction more closely.

Searches for VBF Higgs production with decay into b-quarks without the associated photon requirement have been performed by both ATLAS and CMS. In the all-hadronic channel, ATLAS measured a signal strength, or the ratio between the observed signal yield and that predicted by the Standard Model, of $0.95^{+0.38}_{-0.36}$ [4]. In a boosted (high transverse momentum p_{T}) VBF $H(\to b\bar{b})$ search, CMS measured a signal strength of $4.9^{+1.9}_{-1.6}$ [5]. This letter presents an analysis of $133\,\text{fb}^{-1}$ of $\sqrt{s} = 13\,\text{TeV}$ proton–proton (pp) collision data collected with the ATLAS detector in search of the VBF $H(b\bar{b}) + \gamma$ signature. The VBF Higgs boson signal with the requirement of an associated photon with transverse momentum of at least 19 GeV and two additional jets (VBF Hγjj) with transverse momentum of at least 15 GeV has a cross-section of $55.6^{+0.6}_{-0.4}$ fb predicted at next-to-leading order (NLO). A previous search for this signature using the same dataset observed a signal strength of $\mu_H = 1.3 \pm 1.0$, with an expected significance of 1.0 standard deviations (1.0σ) [6]. Since the previous effort, the multivariate analysis technique has been markedly improved, replacing the previously used boosted decision tree (BDT) classifier with a densely connected neural network (NN) and including the discriminating power of kinematic input variables related to the di-b-jet invariant mass [7]. The data-fitting approach is also quite different from that adopted previously; it now extracts the signal strength directly from the classifier's output score

[1] Authors are listed at the end of this paper.

https://doi.org/10.1016/j.physletb.2026.140279
Received 18 September 2025; Received in revised form 22 January 2026; Accepted 13 February 2026
Available online 9 March 2026

distribution and uses the di-b-jet invariant mass (m_{bb}) to define regions of purity, rather than fitting the m_{bb} distribution. These advances, combined with much larger simulated event samples for the main backgrounds, reduce the signal strength uncertainty and provide improved signal sensitivity.

Details of the analysis procedure are provided in the following sections. Attributes of the experimental detector are given in Section 2. Particulars of the simulated data are presented in Section 3. Characteristics of data collection and event reconstruction and selection are delineated in Section 4. The techniques for separating this rare signal from common backgrounds are described in Section 5, followed in Section 6 with the specifics of ensuring that such backgrounds suitably model the data. Systematic uncertainties related to theory modelling and experimental detector effects are catalogued in Section 7, and the results are presented in Section 8.

2. ATLAS detector

The ATLAS experiment [8] at the Large Hadron Collider (LHC) is a multipurpose particle detector with a forward–backward symmetric cylindrical geometry and nearly 4π coverage in solid angle.[1] It consists of an inner tracking detector surrounded by a thin superconducting solenoid providing a 2 T axial magnetic field, electromagnetic and hadronic calorimeters, and a muon spectrometer. The inner tracking detector covers the pseudorapidity range $|\eta| < 2.5$. It consists of silicon pixel, silicon microstrip, and transition radiation tracking detectors. Lead/liquid-argon (LAr) sampling calorimeters provide electromagnetic (EM) energy measurements with high granularity within the region $|\eta| < 3.2$. A steel/scintillator-tile hadronic calorimeter covers the central pseudorapidity range ($|\eta| < 1.7$). The endcap and forward areas are instrumented with copper/LAr and tungsten/LAr calorimeters for EM and hadronic energy measurements in the region $3.2 \le |\eta| \le 4.9$. The muon spectrometer surrounds the calorimeters and is based on three large superconducting air-core toroidal magnets with eight coils each. The field integral of the toroids ranges between 2.0 and 6.0 T m across most of the spectrometer. The muon spectrometer includes a system of precision tracking chambers up to $|\eta| = 2.7$ and fast detectors for triggering up to $|\eta| = 2.4$. The luminosity is measured mainly by the LUCID-2 detector, which is located close to the beampipe. A two-level trigger system is used to select events [9]. The first-level trigger (L1) is implemented in hardware and uses a subset of the detector information to accept events at a rate below 100 kHz. This is followed by a software-based trigger (HLT) that reduces the accepted event rate to around 1.25 kHz on average depending on the data-taking conditions. A software suite [10] is used in data simulation, in the reconstruction and analysis of real and simulated data, in detector operations, and in the trigger and data acquisition systems of the experiment.

3. Monte Carlo event simulation samples

Fully simulated $H(\to b\bar{b}) + \gamma$ Monte Carlo (MC) signal events were generated at NLO in QCD with MadGraph5_aMC@NLO [11] and showered using Herwig 7 [12,13], with the PDF4LHC15 parton distribution function (PDF) set [14]. This signal sample consists of Higgs bosons produced through VBF or VH processes. The set of tuned parameters is assigned the Herwig 7 default values of H7-PS-MMHT2014LO and H7-UE-MMHT. Contributions from Higgs processes that are rarer in the selected phase space were considered separately but are treated as background. To describe the $H + \gamma$ component of other Higgs production processes, photon-filtered samples are derived from inclusive productions samples. The ggH sample used Powheg [15–17] interfaced with Pythia 8 [18]. Higgs production in association with a $t\bar{t}$ pair (ttH) is described with MC simulated events also generated using Powheg interfaced with Pythia 8 and the NNPDF3.0 PDF set [19].

Table 1
Generators, orders of calculation, and PDF sets used for the MC signal and background samples. The short name of aMC@NLO is used for MadGraph5_aMC@NLO.

Sample	Generator	Calculation order	PDF set
$H(\to b\bar{b}) + \gamma$	aMC@NLO + Herwig 7	NLO	PDF4LHC15
$ggH + \gamma$	Powheg NNLOPS + Pythia 8	NNLO	PDF4LHC15
ttH (all-hadronic)	Powheg + Pythia 8	NNLO	NNPDF3.0
ttH (semileptonic)	Powheg + Pythia 8	NNLO	NNPDF3.0
$Z(\to b\bar{b})\gamma jj$ (EWK)	aMC@NLO + Herwig 7	NLO	PDF4LHC15
$Z(\to b\bar{b})\gamma jj$ (QCD)	MadGraph5 + Pythia 8	LO	PDF4LHC15
$b\bar{b}\gamma jj$ (non-resonant)	MadGraph5 + Pythia 8	LO	PDF4LHC21
$c\bar{c}\gamma jj$ (non-resonant)	MadGraph5 + Pythia 8	LO	PDF4LHC21
$t\bar{t}$ (non-all-hadronic)	Powheg + Pythia 8	NLO	NNPDF3.0
$t\bar{t}$ (all-hadronic)	Powheg + Pythia 8	NLO	NNPDF3.0

For the main non-resonant backgrounds, $b\bar{b}\gamma jj$ and $c\bar{c}\gamma jj$, large samples of fully-simulated Monte Carlo background events were generated at leading order (LO) specifically for this analysis, using MadGraph5_aMC@NLO for the matrix element calculation and Pythia 8 for the showering to final-state particles. Both of these samples used the PDF set PDF4LHC21 [20], and a restriction requiring dijet invariant mass above 500 GeV was applied to improve event selection efficiency in the 'offline' phase space discussed in Section 4. This truth-level dijet invariant mass requirement selects about 37% of all non-resonant QCD background events, which are then passed to the detailed detector simulation, without biasing the results. No events with truth-level invariant mass below 500 GeV have reconstructed-level invariant mass passing the offline requirement (> 800 GeV) described in the next section. The final non-resonant background considered, $t\bar{t}$ production, is modelled by samples with all-hadronic or either partially or fully leptonic final states that were generated at NLO using Powheg and showered using Pythia 8. These samples were normalized to the next-to-next-to-leading order (NNLO) cross-section predictions [21]. Electroweak $Z\gamma jj$ events were modelled specifically for this analysis at NLO using the same parameter values and PDF set as the signal sample. QCD $Z\gamma jj$ events were generated at LO using MadGraph5_aMC@NLO for the hard-scattering and Pythia 8 for showering.

Certain simulation configurations are common to all samples. The decays of bottom and charm hadrons were performed by EvtGen [22]. Fully simulated minimum-bias events were generated using the Pythia 8 generator [23] with the NNPDF2.3lo PDF set and the A3 set of tuned parameters [24], and then overlaid on each hard-scatter interaction, in accord with the luminosity profile of the recorded data, to model pileup contributions from the same bunch crossing and neighbouring bunch crossings. All simulated samples include a full simulation of the ATLAS detector and its response [25] based on Geant4 [26]. Generator choices, the orders of their calculations, and PDF sets used for the considered MC samples are summarized in Table 1.

4. Object and event selection

The target signature of this analysis consists of two jets passing the requirements of a flavour-tagging algorithm ('b-tagged jets') from the b-quarks from the Higgs boson decay, of two additional jets ('VBF-candidate jets') with large invariant mass originating from the quarks that produced the hard scattering after the emission of the W or Z

[1] ATLAS uses a right-handed coordinate system with its origin at the nominal interaction point (IP) in the centre of the detector and the z-axis along the beam pipe. The x-axis points from the IP to the centre of the LHC ring, and the y-axis points upwards. Polar coordinates (r, ϕ) are used in the transverse plane, ϕ being the azimuthal angle around the z-axis. Tranverse momentum (p_T) and energy (E_T) are the components of momentum and energy in this transverse plane, perpendicular to the beamline. The pseudorapidity is defined in terms of the polar angle θ as $\eta = -\ln\tan(\theta/2)$ and is equal to the rapidity $y = \frac{1}{2}\ln\left((E+p_z)/(E-p_z)\right)$ in the relativistic limit. Angular distance is measured in units of $\Delta R \equiv \sqrt{(\Delta y)^2 + (\Delta\phi)^2}$.

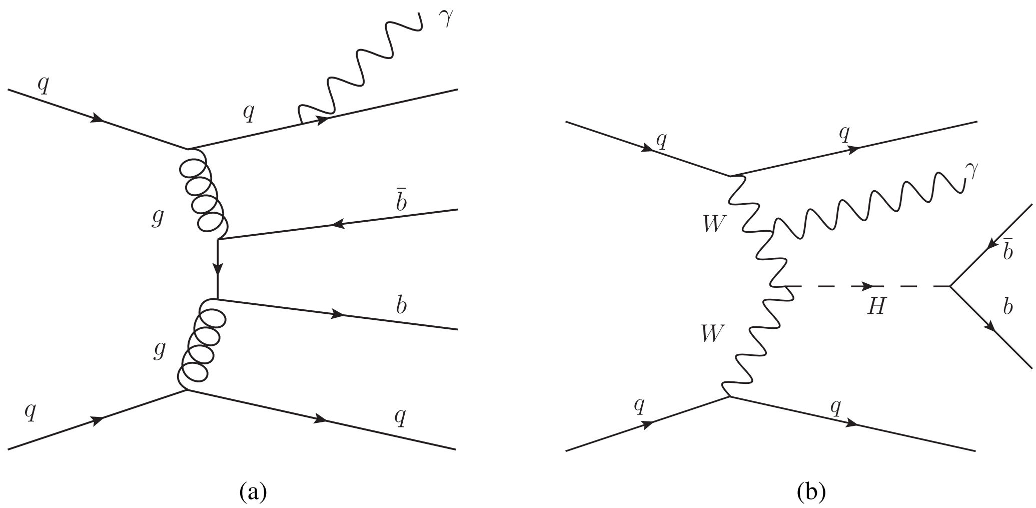

Fig. 1. Representative Feynman diagrams for (a) non-resonant multijet background and (b) $H\gamma jj$ signal. The non-resonant multijet background can also have a qg initial state, and the photon can be radiated from an initial-state or final-state quark.

bosons that fused into a Higgs boson, and of a high-energy photon candidate. Isolated leptons are vetoed to maintain orthogonality with other ATLAS Higgs boson analyses. The selection requirements for these objects, which balance high signal acceptance with high background rejection, are summarized in Table 2.

This analysis uses the full Run-2 dataset recorded from 13 TeV pp collisions by the ATLAS detector from 2015 to 2018. Several triggers were chosen and combined to target the VBF phase space and maximize the acceptance. One motivation for requiring an associated photon in this Higgs boson search is the clean signature the photon provides for triggering, so each trigger chosen in the HLT requires at least one central photon with $p_T > 25$ GeV [27]. These triggers also require at least four jets with $p_T > 35$ GeV. Since the VBF topology tends to produce final-state jets with large angular separation and high invariant mass, the triggers required the largest dijet mass to be at least 700 GeV. Starting from late 2016, these triggers also required at least one jet to be b-tagged at the 77% efficiency working point of the MV2c20 or MV2c10 algorithm [28]. Because of changes in trigger availability and data-quality requirements [29], particularly in the early Run-2 period, this analysis uses a total integrated luminosity of 133 fb^{-1}, slightly less than the 140 fb^{-1} used in other ATLAS full Run-2 analyses.

Interaction vertices from pp collisions are reconstructed from at least two tracks with $p_T > 500$ MeV that are consistent with originating from the beam collision region. If more than one interaction vertex is found in the event, the vertex with the largest sum of track squared p_T is selected as the primary vertex [30]. Due to trigger requirements, each of the four jets selected offline are required to have $p_T > 40$ GeV. Jets are reconstructed using the anti-k_t algorithm [31,32] with a radius parameter of $R = 0.4$, using as inputs 'particle flow' objects determined by matching the energy deposits in the calorimeter with tracks in the inner detector. This choice of particle flow objects leads to better resolution and pileup rejection [33] compared to Ref. [6], for which the jet clustering inputs were topological clusters of neighbouring cells in the calorimeters with significant energy deposits. To enhance pileup rejection, jets in the central region must be tightly matched to the event's primary vertex according to a likelihood-based discriminant called the jet-vertex tagger (JVT), while the similar forward jet-vertex tagger accepts a looser matching for jets in the forward region [34,35].

This analysis replaces the MV2c10 offline b-tagging algorithm, used in the previous analysis [6], with the more advanced DL1r algorithm, which employs a deep neural network for jet flavour classification [36]. The pseudorapidity of b-tagged jets must fall within the acceptance of the inner detector ($|\eta| < 2.5$), on which flavour-tagging heavily relies. Jets are b-tagged if they pass a fixed-cut working point of the DL1r tagging discriminant, which was calibrated using $t\bar{t}$ events to give 77% efficiency for true b-jets with $p_T \geq 20$ GeV. The 77% efficiency working point provides rejection factors of 6 and 134 for charm and light-flavour jets, respectively. Per-jet scale factors are applied in MC events to account for efficiency differences between data and simulation [37–39]. In the simulation, b-tagging is fully emulated ('direct tagging') for all jets for signal events and for events from background processes other than $b\bar{b}\gamma jj$ and $c\bar{c}\gamma jj$. Simulated events that do not have at least two b-tagged jets are rejected outright. In contrast, the two main backgrounds, $b\bar{b}\gamma jj$ and $c\bar{c}\gamma jj$, undergo 'truth-tagging' to maximize the number of simulated events used in the subsequent steps of the analysis. Each event is assigned a weight based on the probability of each jet in the event to pass or fail the b-tagging requirement based on their kinematic properties and flavour of the originating quark. These tagging approaches yield kinematic distributions that differ negligibly in shape, but noticeably in normalization due to the online b-tagging trigger requirement which forces a direct-tagging scheme for at least one of the b-jet candidates [40]. This normalization effect is unimportant because the normalization of these two backgrounds combined is determined by a fit to data, as described in Section 6. To compensate for b-jet energy losses due to semileptonic decays and small out-of-cone energy deposits, jet energy corrections are applied, including corrections for muons or undetected neutrinos from such decays [41]. The two b-tagged jets with highest transverse momentum are selected as Higgs boson decay-product candidates. The remaining jets with p_T greater than 40 GeV are combined pairwise, and the VBF-candidate jets are selected as the pair with the highest invariant mass, requiring that this mass exceeds 800 GeV, where the trigger efficiency reaches a plateau.

The high-energy photon in the signal signature is the photon candidate with highest transverse momentum, with minimum $p_T \geq 30$ GeV and pseudorapidity in the range $|\eta| < 1.37$ or $1.52 < |\eta| < 2.37$. Photons are reconstructed from topological clusters of neighbouring cells in the electromagnetic calorimeter, not matched or matched to tracks in the inner detector depending on whether the photon underwent a conversion to e^+e^- prior to reaching the calorimeter. A tight photon identification selection, based on shower-shape criteria is applied to avoid selecting misidentified electrons or jets reconstructed as photons [42]. Photon isolation requirements set an upper bound on the energy deposited in the calorimeter in a cone surrounding the photon, further helping to reject jets faking prompt photons.

Electron candidates must satisfy $p_T > 25$ GeV, $|\eta| < 2.47$, and tight identification criteria [42]. Muon candidates must satisfy $p_T > 25$ GeV

Table 2
Trigger and offline event selection criteria and region definitions for the $H(\to b\bar{b})jj+\gamma$ signature. The p_T and $|\eta|$ offline jet requirements are used to match trigger selections and b-tagging requirements. Criteria in m_{bb} define the control and signal regions.

Trigger	L1	≥ 1 photon with $p_T > 22$ GeV
	HLT	≥ 1 photon with $p_T > 25$ GeV ≥ 4 jets with $p_T > 35$ GeV and $\|\eta\| < 4.9$ (or ≥ 3 jets with $\|\eta\| < 4.9$ and ≥ 1 b-tagged jet with $\|\eta\| < 2.5$) $m_{jj} > 700$ GeV
Offline		≥ 1 photon with $p_T > 30$ GeV and $\|\eta\| < 1.37$ or $1.52 < \|\eta\| < 2.37$ ≥ 2 b-tagged jets with $p_T > 40$ GeV and $\|\eta\| < 2.5$ ≥ 2 additional jets with $p_T > 40$ GeV and $\|\eta\| < 4.5$ $m_{jj} > 800$ GeV No electrons or muons with $p_T > 25$ GeV $m_{bb} \leq 220$ GeV
Region selection	Signal region	$100\text{ GeV} \leq m_{bb} \leq 150\text{ GeV}$
	Control region	$m_{bb} < 100$ GeV and $150\text{ GeV} < m_{bb} \leq 220$ GeV

and loose identification criteria [43]. For electrons, track-based isolation requirements depend on the electron's p_T, using tracks within a variable cone size of up to $\Delta R = 2$. The calorimeter-based isolation requires that the sum of cluster transverse energies within a cone of $\Delta R = 2$ is less than 3.5 GeV. For muons, the isolation requirement is that tracks within a cone of size $\Delta R = 0.2$ around the muon candidate track must sum to less than 1.25 GeV in p_T. Any events containing isolated electrons or muons with $p_T > 25$ GeV are vetoed. Electron (muon) candidates are matched to the primary vertex by requiring that the significance of their transverse impact parameter d_0 satisfies $|d_0/\sigma(d_0)| < 5.0$ (3.0), where $\sigma(d_0)$ is the measured uncertainty in d_0, and by requiring that their longitudinal impact parameter $z_0 \sin(\theta)$ satisfies $|z_0 \sin(\theta)| < 0.5$ mm.

To reduce instances of considering the same physics object as two different reconstructed objects, an overlap removal is performed after the kinematic criteria for object selection are met. First, any jet within $\Delta R = 0.2$ of an electron is removed, and a jet with fewer than three associated tracks is removed if it is within $\Delta R = 0.2$ of a muon. Any remaining electrons or muons found within $\Delta R = 0.4$ of a jet are then removed. Then, any photon identified within $\Delta R = 0.4$ of an electron or muon is removed. Finally, any jet that is within a region of $\Delta R = 0.4$ around a photon with $p_T > 30$ GeV is removed, as it is likely to have been reconstructed from the same energy deposits as the photon candidate.

After the event selection criteria have been applied, candidate events are divided into two regions, which are used together in the classifier training and in the signal extraction fit. The signal region (SR) contains most of the signal sensitivity, comprising events with m_{bb} in the range $100\text{ GeV} \leq m_{bb} \leq 150$ GeV around the Higgs boson mass. The control region (CR) includes events in the m_{bb} sidebands outside this window, specifically $m_{bb} < 100$ GeV and $150\text{ GeV} < m_{bb} \leq 220$ GeV. It is primarily used to extract background normalizations and to constrain nuisance parameters representing correlated systematic uncertainties.

5. Multivariate analysis

An improved multivariate analysis technique is key to this analysis. An NN replaced the BDT used in the previous analysis because the NN showed better signal and background discrimination with identical inputs. KERAS [44], a high-level interface of TENSORFLOW [45], was used to train an NN to provide a classification score, distinguishing signal-like (high score) events from those resembling the non-resonant QCD $b\bar{b}\gamma jj$ or $c\bar{c}\gamma jj$ events constituting the main backgrounds (low score). A two-fold method was used to train and evaluate the performance of the NN: two separate models with identical hyperparameters were trained on separate halves of the MC training samples, which contain both the control- and signal- region phase spaces. Evaluating the MC events using the model that did not include those events during training allows the use of the full size of the MC samples for signal extraction. Data and MC background samples that were not used in training are also split in half, and the two halves are evaluated by each of the two models and then recombined.

In order to optimize the choice of input variables and hyperparameters, a comparison metric was formed to assess the signal-background separation significance after successive training epochs. The significance is estimated by binning the NN output score distribution into 20 bins, equal in width in score, and the weighted number of signal events is divided by the square root of the weighted number of background events ($S/\sqrt{B}$) in each bin. The optimization metric is these $S/\sqrt{B}$ values summed in quadrature for all bins. Many kinematic variables were considered as inputs; combinations of these variables were used to train individual models, which were evaluated using the defined metric to find the optimal set. After optimization, the 14 input variables listed in Table 3 were selected, and no addition or substitution made to this grouping was found to produce better separation between signal and background. In addition to the improvements gained from the use of an NN, this analysis profits from the use of the discriminating power of m_{bb} and correlated variables, which could not be exploited in the previous analysis because it would sculpt the background parametrization. The use of variables related to an event's jet multiplicity is also a new development, motivated by the signal's tendency, with mostly electroweak vertices, to have fewer jets than the QCD background. The same optimization method was employed to select specific hyperparameter settings: each final NN model has 11 hidden layers with 256 neurons per layer in the bulk. The ratio of the sums of weights of the background and signal training samples was also optimized, after which the signal acceptance contributed more than twice as much as the background rejection to the loss function. To prevent overtraining, the training is stopped when the calculated loss function does not decrease significantly for five consecutive training epochs, which typically occurs within 25 epochs for the final selection of hyperparameters.

6. Signal and background composition and modelling

The previous analysis of this signature with the full Run-2 data relied on a fit to the invariant mass spectrum of the two b-tagged jets (m_{bb}), using an analytic shape for the background, with parameters determined from the fit to the data. That approach introduced large systematic uncertainties from the potential bias arising from the choice of the model for the background. This analysis adopts a binned likelihood fitting strategy to the NN score, based on signal and background templates derived from MC simulations, reducing modelling-related systematic uncertainties and benefitting from the use of a more discriminating variable as the fit observable.

Simulations and calculations of the SM cross-sections predict that non-resonant backgrounds are expected to contribute approximately

Table 3
Kinematic variables used as inputs to the neural-network classifier. This list is ordered in decreasing correlation between the input variable and the NN score, i.e. in decreasing order of importance in the NN training.

Input variable	Description
n_{jets}	The total number of jets with $p_{\text{T}} \geq 40\,\text{GeV}$ in the event
$p_{\text{T}}^{\text{bal}}$ [6]	Transverse momentum balance for selected final-state objects
$\Delta\phi(bb,jj)$	Azimuthal angle between the momenta of the di-b-jet system and the two VBF-candidate jets
m_{bb}	Invariant mass of the two leading b-tagged jets
p_{T}^{bb}	Transverse momentum of the two leading b-tagged jets
m_{jj}	Invariant mass of the two VBF-candidate jets
$\cos\theta_C$	Cosine of the angle between the two VBF-candidate jets and the two b-tagged jets planes in the centre-of-mass frame of the $bbjj$ system
$\min(\Delta R(b,\gamma))$	The minimum angular distance between one of the b-tagged jets and the photon
$\Delta\eta(j,j)$	Pseudorapidity difference between two VBF-candidate jets
$\Delta R(b_1,j_1)$	Angular distance between the leading b-tagged jet and the leading VBF-candidate jet
$p_{\text{T}}^{j_1}$	Transverse momentum of the leading VBF-candidate jet
cen(γjj) [6]	Centrality of the photon relative to the VBF-candidate jets
$\Delta\eta(b,b)$	Pseudorapidity difference between the two leading b-tagged jets
η_{j_5}	Pseudorapidity of a 5th jet (2 b-tagged jets, 2 VBF-candidate jets, plus this extra 5th jet); if no 5th jet is present, a value is assigned using a probability density matching the distribution of 5-jet events from the respective sample population

99% of the total background. Prior to any constraints from a fit to data, QCD multijet production with b-quarks in association with a photon ($b\bar{b}\gamma jj$) dominates with a 70% contribution, multijet production with mistagged c-quarks in association with a photon ($c\bar{c}\gamma jj$) contributes an estimated 18%, and non-resonant production of top quarks ($t\bar{t}$) is estimated to contribute 11% of the total expected background. Non-resonant QCD production with light-flavour quarks in association with a photon ($l\bar{l}\gamma jj$) is conservatively estimated to contribute $< 0.5\%$ of the total background yield based on the mistagging rate for light-flavour jets, so no template for this background source is included.

Although resonant backgrounds are estimated to contribute only 1% of the total background, templates are still produced and included in the fit because the kinematics of resonant backgrounds are more similar to signal than to the non-resonant backgrounds. The template for the background from Z boson production in association with a photon and jets, $Z(\rightarrow b\bar{b})\gamma jj$, is built from the sum of two contributions, electroweak and QCD production, as described in Section 3. The contribution from $W\gamma$ production is estimated to be only 1% of that from $Z\gamma$ after selection, so no template is included in the fit for $W\gamma jj$. Other Higgs production modes contribute negligibly to the selected phase space, due to the required associated photon and the VBF-specific event selections. Nevertheless, templates are created for ggH and $t\bar{t}H$ production, which is treated as background to the predominantly VBF Higgs signal.

While this analysis focuses on the VBF $H\gamma$ production mode of the $bb\gamma jj$ signal, $VH\gamma$ contributes an estimated 8.8% of the signal sample at MC generator level, but it is expected to contribute less than 1% after final event selection phase-space requirements. Of the signal VBF events at generator level, about 92.3% are estimated to be from Higgs boson production via WW-fusion, due to production via ZZ-fusion being suppressed by the interference effect mentioned in Section 1.

The templates for the $b\bar{b}\gamma jj$ and $c\bar{c}\gamma jj$ backgrounds use 'truth-tagging' to benefit from as many of the MC events as possible, and tests were performed to ensure that the NN output distribution shapes are compatible with direct-tagged sample templates [40]. These two backgrounds share a floating normalization factor, allowing their combined yield to be fitted directly to data. The remaining background and signal templates use direct-tagged samples. While truth-tagged MC signal events are used in the NN training to have ample training samples, the signal fit template is derived by evaluating the NN on only direct-tagged events.

As mentioned in Section 1, the fitting strategy extracts the signal directly from the NN output score distribution, and uses a control region and signal region defined by ranges in m_{bb}. This fit relies on template distributions derived from MC, so it is important to ensure that the MC background simulation agrees well with data in the control region where there is little signal contamination. In this control region, discrepancies between data and MC simulation are observed for several kinematic variables, particularly n_{jets}, $\min(\Delta R(b,\gamma))$, $\Delta\eta(j,j)$, and m_{bb}. This was also observed in Ref. [6], and is due to both the difficulty of modelling non-resonant multijet backgrounds and the low order at which the dominant MC samples were generated.

To achieve better agreement between data and MC events in the NN output distribution and to account for possible missing backgrounds such as events arising from jets improperly tagged as photons, reweighting scale factors for the two main background, $b\bar{b}\gamma jj$ and $c\bar{c}\gamma jj$, are extracted from distributions of the 14 NN input kinematic variables listed in Table 3. These backgrounds are reweighted together with identical kinematic scale-factor functions as follows. After the MC-estimated $t\bar{t}$ contribution is subtracted, the data are compared with the predicted $b\bar{b}\gamma jj + c\bar{c}\gamma jj$ background, via the ratio of the normalized binned kinematic input-variable distributions in the m_{bb}-sideband control region. To this ratio, a sixth-order polynomial is fitted successively and iteratively for each input variable, in the reverse order of their correlation with NN score. The function is then applied to the MC $b\bar{b}\gamma jj$ and $c\bar{c}\gamma jj$ samples, in both the control region and signal regions, in order to scale these dominant backgrounds to better represent the data. These kinematic reweighting scale factors account for any mismodelling of these non-resonant QCD backgrounds, as well as for any contamination from backgrounds not otherwise considered, such as jets misidentified as photons.

The NN training is repeated after kinematic reweighting to obtain the final model, such that the modified event weights can affect the loss function and training results accordingly. Despite the large number of compounding scale factors, the overall impact on the NN output is relatively small because their effects partially cancel. Additionally, the reweighted result is largely immune to procedural changes, as reflected in the shape uncertainty due to this kinematic reweighting (see Section 7). Very good closure between MC and data distribution shapes after kinematic reweighting can be seen in the control region and the background-rich areas of the signal region, i.e. in the m_{bb} SR window $100 \leq m_{bb} \leq 150$ GeV but with an NN score less than 0.6. Fig. 2 shows the NN output distributions for the MC backgrounds before and after kinematic reweighting in comparison with data in the control region and signal region. In the CR and in the background-rich bins of the SR, the data and reweighted MC distributions agree within statistical uncertainties.

7. Systematic uncertainties

Theory and experimental uncertainties are described with a total of 78 nuisance parameters that can modify the normalization and shape of the signal and background templates. The effects of these nuisance parameters on the signal strength uncertainty ($\sigma(\mu_H)$) are categorized and summarized in Table 4. The grouped effect of each uncertainty category is calculated by performing a fit with the category's corresponding nuisance parameters fixed to their best-fit values, and taking the difference in quadrature between $\sigma(\mu_H)$ from the nominal fit and from this fit as the impact of that group of systematic uncertainties. Template smoothing is employed in these final-fit variations to reduce the inflation of uncertainties due to correlated statistical fluctuations.

The dominant source of signal strength uncertainty is the statistical uncertainty, which contributes $\sigma(\mu_H) = 0.57$. This is due to the small $H+\gamma$ production cross section at $\sqrt{s} = 13\,\text{TeV}$. Nevertheless, much attention was paid to reducing the experimental and modelling uncertainties as much as possible relative to the previous analysis. To reduce the statistical uncertainties of the background templates, new and enlarged

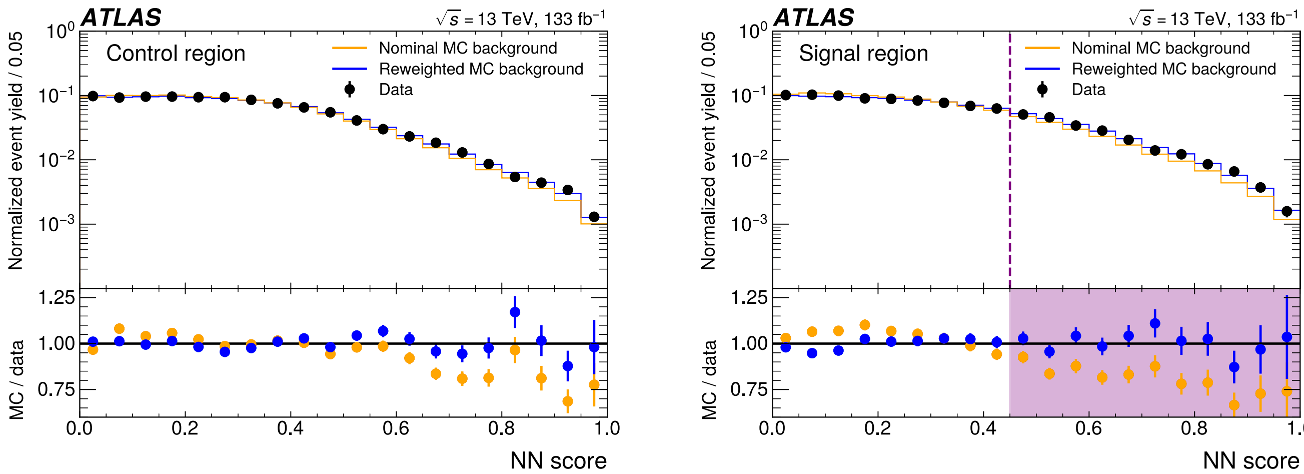

(a) (b)

Fig. 2. NN output distributions for data compared with those for all MC backgrounds with and without kinematic reweighting. Reweighting scale factors are extracted from comparisons between kinematic distributions for MC backgrounds and data in the (a) control region m_{bb} sidebands. The low score bins of the (b) signal region, which have negligible signal, are used for validation. The purple dashed line marks the divide between the low-score SR bins, used for validation of the reweighting scale factors, and high-score bins containing most of the signal. The total yields of MC and data events are individually normalized to 1, making this a direct comparison of NN output distribution shapes.

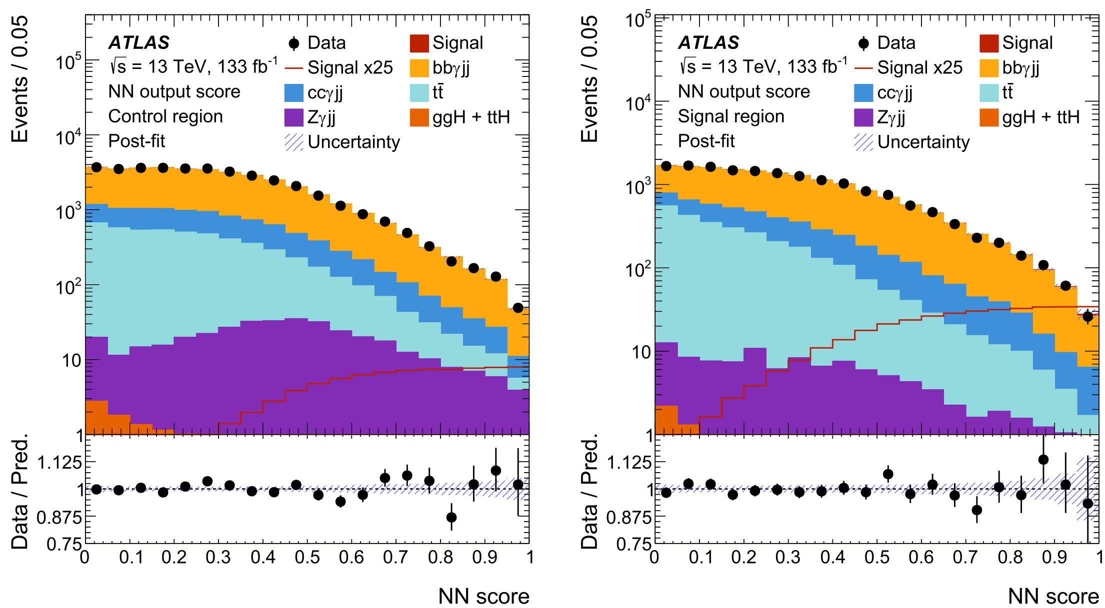

(a) (b)

Fig. 3. Post-fit plots for the observed dataset, showing (a) the control region and (b) the signal region. Background and signal templates are shown with all normalization factors and post-fit nuisance parameter pulls incorporated. Data bin yields are represented with black markers, with error bars representing statistical uncertainties. The red line represents the post-fit signal scaled by a factor of 25, while the stacked red signal histogram, which is only visible at high NN score in the signal region, is normalized to the fitted signal strength of $\mu = 0.2$. The ratio plots in the lower panels display the bin-by-bin ratio of the data to the post-fit total of signal and background yields. Post-fit uncertainties are depicted with a blue hashed band in both the yield and ratio plots. The NN score is renormalized in the post-fit distributions to give regular bin widths, so the binning does not reflect the raw score optimized binning, which is finer in high score signal region bins and low score control region bins.

$b\bar{b}\gamma jj$ and $c\bar{c}\gamma jj$ samples were simulated; these reduced the MC statistical uncertainty contributions to a total of $\sigma(\mu_H) = 0.25$.

Theory uncertainties arising from the lack of higher-order corrections, the PDF and α_s, and the parton shower generator are considered for the signal and major backgrounds. To estimate the contributions from missing higher-order corrections in the calculations, an envelope of the effects of varying the chosen renormalization and factorization scale values is used. The dominant normalization uncertainties of the $b\bar{b}\gamma jj$ and $c\bar{c}\gamma jj$ backgrounds come from this variation of the renormalization scale μ_R and the factorization scale μ_F. MC events were reweighted in accord with changes in these QCD scales, leading to a change of roughly +60% and −40% in the yield for each sample, independent of NN score. The effects of a seven-point variation, $(\{\mu_R, \mu_F\} \times \{0.5, 0.5\}, \{1.0, 0.5\}, \{0.5, 1.0\}, \{1.0, 1.0\}, \{1.0, 2.0\}, \{2.0, 1.0\}, \{2.0, 2.0\})$, is

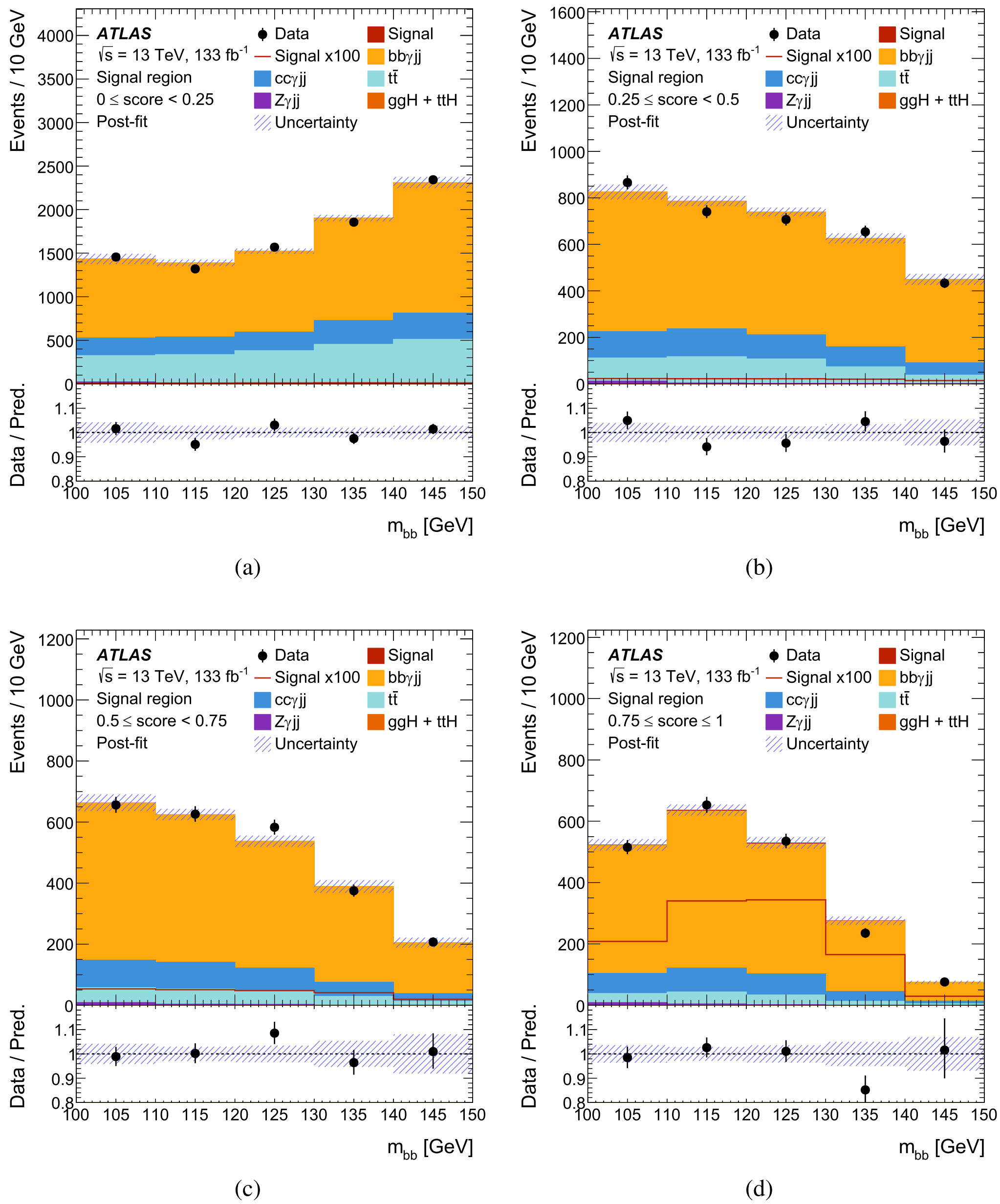

Fig. 4. Post-fit signal region m_{bb} distributions in slices of NN score. Stacked histograms represent post-fit MC background and signal, and the black markers with error bars represent data. The red lines represent post-fit signal distributions scaled by a factor of 100. The stacked red histogram, which can only be visualized in some bins of the highest NN score slice, is normalized to the post-fit signal strength, $\mu = 0.2$. The lower panels show the ratio of data to post-fit MC signal plus background. Post-fit uncertainties are depicted by blue hashed lines.

taken as the systematic uncertainty, including both the cross-section and acceptance uncertainties. Shape effects from these scale variations are not large, but are included and treated as being uncorrelated with the normalization effects to avoid a degeneracy between these nuisance parameters and the floating normalization factor. The scale-uncertainty nuisance parameters for $b\bar{b}\gamma jj$ and $c\bar{c}\gamma jj$ are assumed to be uncorrelated as well, despite their production processes being similar, and in doing so, the ratio of the yields of the two samples is given a large range of freedom.

The uncertainties due to missing higher orders for the signal are evaluated in the same way as for the background, but they are found to be much smaller, about 1%, and correlation between normalization and shape components is allowed in the fit. For the $t\bar{t}$ background, the uncertainty in the cross-section estimated at NNLO in QCD [46] is used to account for QCD scale-variation effects, and thus an overall relative uncertainty of $^{+2.5\%}_{-3.6\%}$ is assigned to the $t\bar{t}$ background. For the small $Z\gamma jj$ background, a conservative estimate of $\pm 16\%$ is adopted for the overall magnitude of scale-variation effects, matching the uncertainty estimated in Ref. [47].

Systematic uncertainties due to the choice of PDF and α_s are estimated by reweighting probability densities at the event level. For signal, 42 members of the set PDF4LHC15 are considered, including 40 PDF eigenvariations along with α_s variations upward and downward by 1 standard deviation. The uncertainty is calculated as the sum in quadrature of the effects of these variations [14], which leads to an uncertainty of 2.2% for signal. For $b\bar{b}\gamma jj$ and $c\bar{c}\gamma jj$, 100 PDF variations of the set PDF4LHC21 are considered, and the uncertainty is computed as the standard deviation of the yields from each variation. This PDF uncertainty is combined in quadrature with the change in yield from the average of the upward and downward α_s variations. The resulting

Table 4
The observed impacts of the statistical, theory, and experimental uncertainties on the signal strength uncertainty, as extracted from the final fit to observed data. Data statistical uncertainty is the single largest contribution to the total uncertainty.

Source of uncertainty	$+\sigma(\mu_H)$	$-\sigma(\mu_H)$
Statistical Data sample size	+0.57	−0.56
MC background templates	+0.25	−0.22
Theory and modelling Kinematic reweighting	+0.07	−0.06
MC modelling	+0.19	−0.15
Background normalization	+0.13	−0.08
Experimental Luminosity	+0.004	−0.006
Jet + photon selection	+0.15	−0.11
b-tagging	+0.03	−0.03
Total	+0.69	−0.64
Total MC statistical	+0.25	−0.22
Total theory	+0.24	−0.18
Total experimental	+0.16	−0.12

PDF and α_s choice uncertainty is 3.2% for $b\bar{b}\gamma jj$ and 3.3% for $c\bar{c}\gamma jj$. The equivalent uncertainty for $t\bar{t}$ production is 2.5%, again taken from the uncertainty in the best prediction of the NNLO cross-section [48]. PDF and α_s uncertainties are not considered directly for the other backgrounds, as such small variations on the rarer backgrounds have negligible impact on the signal measurement. However, for the minor Higgs boson production modes that are treated as backgrounds in this analysis, an overall normalization uncertainty of 20% is introduced to conservatively cover any modelling uncertainties.

The largest shape variation from a single systematic uncertainty source comes from the choice of parton shower generator, giving bin-by-bin variations as large as 5%. For the dominant $b\bar{b}\gamma jj$ and $c\bar{c}\gamma jj$ backgrounds, alternative samples were produced using MadGraph5_aMC@NLO and Herwig, instead of the MadGraph5_aMC@NLO and Pythia combination used in obtaining the nominal templates. These samples were produced at MC truth-level, so a method was designed to extract the truth-level effects of differences between Pythia and Herwig showering and transfer those effects to modifications of the fully simulated NN output distributions. Scale factors are extracted from the ratios of truth-level Pythia and Herwig kinematic distributions for each of the 14 NN input variables (similar to the process for kinematic reweighting discussed in Section 6). These scale factors are then applied to the fully simulated and kinematically reweighted Pythia NN outputs to obtain a facsimile of a fully simulated Herwig NN outputs. The effects of these representative parton shower variations are included as systematic uncertainties with two-sided symmetrization. Separate nuisance parameters were introduced for the signal region and control region for these dominant backgrounds, because the NN output distribution shape is affected differently in the two regions.

For signal, the alternative shower samples were generated with Herwig 7 like the nominal samples but with variations of the hard scale factor by factors of two, which affects the maximum allowed transverse momentum for shower emissions [13]. The method used for transfer from truth-level to proxy fully simulated distributions is the same as described for the two main non-resonant backgrounds, and it results in bin-by-bin variations as large as 20% in signal-sensitive regions. For $t\bar{t}$ production, hard-scatter (matrix element) and parton shower uncertainties are estimated by comparing the nominal samples directly with fully simulated samples generated with MadGraph5_aMC@NLO [5] replacing Powheg and Herwig 7 replacing Pythia 8. The parton shower variation changes the $t\bar{t}$ sample normalization by almost 10%. The effects of the matrix element variation are small in the control region, changing the $t\bar{t}$ normalization by 0.6%, but larger in the signal region, with a normalization change of 5.3%.

The kinematic reweighting of the dominant $b\bar{b}\gamma jj$ and $c\bar{c}\gamma jj$ backgrounds also has associated systematic uncertainties. The reweighting is performed by extracting scale factors from the ratio of the sum of these two simulated backgrounds to the $t\bar{t}$-subtracted data. Thus, the systematic uncertainty is derived by considering how the result of this reweighting changes if the $t\bar{t}$ contribution is overestimated or underestimated within its theoretical uncertainties. Since the scale factors are extracted concurrently for $b\bar{b}\gamma jj$ and $c\bar{c}\gamma jj$ directly in the control region and extrapolated to the signal region, uncertainty is considered only in the signal region and is correlated between the two backgrounds. Due to the robustness of the kinematic reweighting procedure, these $t\bar{t}$ contribution variations have little impact on the NN output distribution's shape. In the unique case of m_{bb}, for which the phase space covered in the signal region is not represented in the control region, the entire reweighting is taken as an uncertainty: a systematic variation without the scale factors derived for m_{bb} is included in the signal region, and the associated nuisance parameter ranks among the highest in terms of impact to the signal strength uncertainty. The combination of these two kinematic reweighting uncertainty nuisance parameters gives a 6 – 7% impact on the signal strength uncertainty.

Experimental systematic uncertainties arise from uncertainties in the integrated luminosity, jet energies and resolutions, electromagnetic object identification and isolation, and b-jet tagging efficiency. These systematic uncertainties are correlated between samples and fit regions via shared nuisance parameters. Due to the uncertainty in the measurement of the integrated luminosity collected by ATLAS [49], an overall normalization uncertainty of 0.83% is applied to every template sample, but this has negligible impact on the final signal strength uncertainty. Systematic uncertainties arising from jet energy scale (JES) and resolution (JER) uncertainties [50] dominate the experimental category with a 13% contribution to the signal strength uncertainty. Experimental uncertainties arising from the identification and isolation of photons and electrons, as well as their energy and its resolution [42], are also considered but have negligible impact. Uncertainties in b-jet tagging efficiency include effects for both online and offline selections [37–39]. The overall background uncertainty arising from b-tagging requirements is about 2 – 3% and fairly independent of NN score for all samples, but variations in both shape and normalization are considered for the signal and dominant background samples. In all, b-jet tagging uncertainties contribute 3% to the signal strength uncertainty.

8. Results

To extract the signal strength, a binned maximum-likelihood fit is performed directly on the neural-network classifier's output distribution using TRExFitter, which is built from HistFactory [51] and RooFit [52]. The signal strength and the floating normalization factor for the sum of the two main non-resonant backgrounds, $b\bar{b}\gamma jj$ and $c\bar{c}\gamma jj$, are extracted [53] by a simultaneous fit of the control and signal regions, which are defined by the invariant mass of the two leading b-tagged jets as described in Section 6.

Both the control region and signal region have 20 NN score bins with widths optimized independently for each region to maximize the signal sensitivity while keeping the total statistical uncertainties low. The optimization results in very fine binning in the high score range of the signal region, where the signal purity is highest, as well as fine binning in the low score range of the control region, where the number of background events is large. The highest-score bins of the signal region have by far the highest signal purity and sensitivity in the fit. The post-fit NN score distributions in the control region and signal region are shown in Fig. 3. The pre-fit and post-fit yields for the MC-simulated backgrounds and signal are listed in Table 5 together with the number of data events.

The Higgs boson signal strength is defined relative to the Standard Model prediction. An inclusive signal strength of $\mu_H = 0.2 \pm 0.7$ is observed, compared to an expected value of 1.0 ± 0.7. This corresponds

Table 5
Pre-fit and post-fit signal and background yields and data yields in the control region, and in the signal region in the sum of the 17 lowest-NN-score bins and individually in the three highest-NN-score bins. The total background yield and its uncertainty are given post-fit.

Yields	CR		SR Bins 0–16		SR Bin 17		SR Bin 18		SR Bin 19	
	Pre	Post	Pre	Post	Pre	Post	Pre	Post	Pre	Post
$b\bar{b}\gamma jj$	30,600	27,400	12,400	11,100	86	78	55	49	23	20
$c\bar{c}\gamma jj$	7400	5100	3200	2200	15	10	9	6	7	5
$t\bar{t}$	4600	4800	2600	2700	4	5	2	2	1	1
$Z\gamma jj$	400	400	100	100	1	1	1	1	0.4	0.4
$ggH + t\bar{t}H$	10	10	8	8	<0.1	<0.1	<0.1	<0.1	<0.1	<0.1
Total background	37700 ± 130		16100 ± 76		94 ± 5		59 ± 4		27 ± 4	
Signal	14	3	41	9	6	1	6	1	6	1
Data	37701		16070		108		61		26	

to an observed significance of 0.3 standard deviations, compared to an expected significance of 1.5 standard deviations. The 95% confidence level exclusion limit for the VBF Hγjj signal cross-section is observed to be 86.5 fb. A likelihood ratio comparison between the observed fit and a saturated model, which has complete freedom for a perfect fit to data, gives a goodness-of-fit p-value of 30%. The final fit's normalization of the dominant backgrounds is about 85% of the leading-order MC estimate. The measured signal strength is compatible with the previous result, with a p-value of 37%. This probability is calculated without considering correlations because the overlap of data events in the signal-sensitive regions of the two analyses is less than 5%.

To further confirm that the background modelling using the MC-derived templates is acceptable, kinematic distributions are compared with data in the signal region, in slices of NN score, with the propagation of post-fit pulls from the fit to NN score. Fig. 4 shows the di-b-jet invariant mass spectrum in four NN score slices of the signal region. The post-fit MC and data spectra agree within their uncertainties, and no divergence in agreement appears at high score.

9. Conclusion

A search was conducted for associated production of a Higgs boson and a high-energy photon. The full Run-2 dataset from 13 TeV proton–proton collisions collected by the ATLAS detector at the LHC is examined, corresponding to an integrated luminosity of 133 fb^{-1}. The search focuses on the $H(\rightarrow b\bar{b}) + \gamma$ final state, the dominant Higgs boson decay mode, and the photon requirement greatly reduces the multijet background. The photon requirement also makes vector-boson fusion the dominant Higgs boson production mode, with events characterized by the additional presence of two well-separated VBF-candidate jets having a high invariant mass. This analysis improves on a previous one in this channel by using updated and extended Monte Carlo background samples, finely optimized multivariate analysis techniques for signal–background separation, and a novel data-fitting approach to measure the signal strength. With these improvements, a signal significance of 1.5σ is expected, nearly 50% higher than the expected significance in the previous full Run-2 analysis. A Higgs boson signal strength of 0.2 ± 0.7 is measured, with an observed significance of 0.3σ.

Data availability

The data for this manuscript are not available. The values in the plots and tables associated to this article are stored in HEPDATA (http://hepdata.cedar.ac.uk)

Declaration of competing interest

The authors declare that they have no known competing financial interests or personal relationships that could have appeared to influence the work reported in this paper.

Acknowledgements

We thank CERN for the very successful operation of the LHC and its injectors, as well as the support staff at CERN and at our institutions worldwide without whom ATLAS could not be operated efficiently.

The crucial computing support from all WLCG partners is acknowledged gratefully, in particular from CERN, the ATLAS Tier-1 facilities at TRIUMF/SFU (Canada), NDGF (Denmark, Norway, Sweden), CC-IN2P3 (France), KIT/GridKA (Germany), INFN-CNAF (Italy), NL-T1 (Netherlands), PIC (Spain), RAL (UK) and BNL (USA), the Tier-2 facilities worldwide and large non-WLCG resource providers. Major contributors of computing resources are listed in Ref. [54].

We gratefully acknowledge the support of ANPCyT, Argentina; YerPhI, Armenia; ARC, Australia; BMWFW and FWF, Austria; ANAS, Azerbaijan; CNPq and FAPESP, Brazil; NSERC, NRC and CFI, Canada; CERN; ANID, Chile; CAS, MOST and NSFC, China; Minciencias, Colombia; MEYS CR, Czech Republic; DNRF and DNSRC, Denmark; IN2P3-CNRS and CEA-DRF/IRFU, France; SRNSFG, Georgia; BMFTR, HGF and MPG, Germany; GSRI, Greece; RGC and Hong Kong SAR, China; ICHEP and Academy of Sciences and Humanities, Israel; INFN, Italy; MEXT and JSPS, Japan; CNRST, Morocco; NWO, Netherlands; RCN, Norway; MNiSW, Poland; FCT, Portugal; MNE/IFA, Romania; MSTDI, Serbia; MSSR, Slovakia; ARIS and MVZI, Slovenia; DSI/NRF, South Africa; MICIU/AEI, Spain; SRC and Wallenberg Foundation, Sweden; SERI, SNSF and Cantons of Bern and Geneva, Switzerland; NSTC, Taipei; TENMAK, Türkiye; STFC/UKRI, United Kingdom; DOE and NSF, United States of America.

Individual groups and members have received support from BCKDF, CANARIE, CRC and DRAC, Canada; CERN-CZ, FORTE and PRIMUS, Czech Republic; COST, ERC, ERDF, Horizon 2020, ICSC-NextGenerationEU and Marie Skłodowska-Curie Actions, European Union; Investissements d'Avenir Labex, Investissements d'Avenir Idex and ANR, France; DFG and AvH Foundation, Germany; Herakleitos, Thales and Aristeia programmes co-financed by EU-ESF and the Greek NSRF, Greece; BSF-NSF and MINERVA, Israel; NCN and NAWA, Poland; La Caixa Banking Foundation, CERCA Programme Generalitat de Catalunya and PROMETEO and GenT Programmes Generalitat Valenciana, Spain; Göran Gustafssons Stiftelse, Sweden; The Royal Society and Leverhulme Trust, United Kingdom.

In addition, individual members wish to acknowledge support from Armenia: Yerevan Physics Institute (FAPERJ); CERN: European Organization for Nuclear Research (CERN DOCT); Chile: Agencia Nacional de Investigación y Desarrollo (FONDECYT 1230812, FONDECYT 1240864, Fondecyt 3240661, Fondecyt Regular 1240721); China: Chinese Ministry of Science and Technology (MOST-2023YFA1605700, MOST-2023YFA1609300), National Natural Science Foundation of China (NSFC - 12175119, NSFC 12275265, NSFC-12075060); Czech Republic: Czech Science Foundation (GACR - 24-11373S), Ministry of Education Youth and Sports (ERC-CZ-LL2327, FORTE

CZ.02.01.01/00/22_008/0004632), PRIMUS Research Programme (PRIMUS/21/SCI/017); EU: H2020 European Research Council (ERC - 101002463); European Union: European Research Council (BARD No. y101116429, ERC - 948254, ERC 101089007), Horizon 2020 Framework Programme (MUCCA - CHIST-ERA-19-XAI-00), European Union, Future Artificial Intelligence Research (FAIR-NextGenerationEU PE00000013), Italian Center for High Performance Computing, Big Data and Quantum Computing (ICSC, NextGenerationEU); France: Agence Nationale de la Recherche (ANR-20-CE31-0013, ANR-21-CE31-0013, ANR-21-CE31-0022, ANR-22-EDIR-0002, ANR-24-CE31-0504-01); Germany: Baden-Württemberg Stiftung (BW Stiftung-Postdoc Eliteprogramme), Deutsche Forschungsgemeinschaft (DFG - 469666862, DFG - CR 312/5-2); Italy: Istituto Nazionale di Fisica Nucleare (ICSC, NextGenerationEU), Ministero dell'Università e della Ricerca (NextGenEU 153D23001490006 M4C2.1.1, NextGenEU I53D23000820006 M4C2.1.1, NextGenEU I53D23001490006 M4C2.1.1); Japan: Japan Society for the Promotion of Science (JSPS KAKENHI JP22H01227, JSPS KAKENHI JP22H04944, JSPS KAKENHI JP22KK0227, JSPS KAKENHI JP23KK0245); Norway: Research Council of Norway (RCN-314472); Poland: Ministry of Science and Higher Education (IDUB AGH, POB8, D4 no 9722), Polish National Agency for Academic Exchange (PPN/PPO/2020/1/00002/U/00001), Polish National Science Centre (NCN 2021/42/E/ST2/00350, NCN OPUS 2023/51/B/ST2/02507, NCN OPUS nr 2022/47/B/ST2/03059, NCN UMO-2019/34/E/ST2/00393, UMO-2020/37/B/ST2/01043, UMO-2021/40/C/ST2/00187, UMO-2022/47/O/ST2/00148, UMO-2023/49/B/ST2/04085, UMO-2023/51/B/ST2/00920); Portugal: Foundation for Science and Technology (FCT); Spain: Generalitat Valenciana (Artemisa, FEDER, IDIFEDER/2018/048, ASFAE/2022/008), Ministry of Science and Innovation (MCIN & NextGenEU PCI2022-135018-2, MICIN & FEDER PID2021-125273NB, RYC2019-028510-I, RYC2020-030254-I, RYC2021-031273-I, RYC2022-038164-I), Ministerio de Ciencia, Innovación y Universidades/Agencia Estatal de Investigación (PID2022-142604OB-C22); Sweden: Carl Trygger Foundation (Carl Trygger Foundation CTS 22:2312), Swedish Research Council (Swedish Research Council 2023-04654, VR 2018-00482, VR 2021-03651, VR 2022-03845, VR 2022-04683, VR 2023-03403), Knut and Alice Wallenberg Foundation (KAW 2018.0458, KAW 2019.0447, KAW 2022.0358); Switzerland: Swiss National Science Foundation (SNSF - PCEFP2_194658); United Kingdom: Leverhulme Trust (Leverhulme Trust RPG-2020-004), Royal Society (NIF-R1-231091); United States of America: U.S. Department of Energy (ECA DE-AC02-76SF00515), Neubauer Family Foundation.

The ATLAS Collaboration

G. Aad[152], E. Aakvaag[18], B. Abbott[174], S. Abdelhameed[169], K. Abeling[82], N.J. Abicht[76], S.H. Abidi[43], M. Aboelela[71], A. Aboulhorma[59], H. Abramowicz[223], Y. Abulaiti[171], B.S. Acharya[100,101,260], A. Ackermann[91], C. Adam Bourdarios[5], L. Adamczyk[134], S.V. Addepalli[213], M.J. Addison[151], J. Adelman[168], A. Adiguzel[26], T. Adye[194], A.A. Affolder[196], Y. Afik[65], M.N. Agaras[14], A. Aggarwal[150], C. Agheorghiesei[36], F. Ahmadov[64,276], S. Ahuja[145], X. Ai[206], G. Aielli[115,116], A. Aikot[236], M. Ait Tamlihat[59], B. Aitbenchikh[55], M. Akbiyik[150], T.P.A. Åkesson[148], A.V. Akimov[215], D. Akiyama[241], N.N. Akolkar[31], S. Aktas[24], G.L. Alberghi[30], J. Albert[238], P. Albicocco[80], G.L. Albouy[88], S. Alderweireldt[79], Z.L. Alegria[175], M. Aleksa[61], I.N. Aleksandrov[64], C. Alexa[35], T. Alexopoulos[11], F. Alfonsi[30], M. Algren[83], M. Alhroob[240], B. Ali[192], H.M.J. Ali[141,269], S. Ali[45], S.W. Alibocus[142], M. Aliev[49], G. Alimonti[105], W. Alkakhi[82], C. Allaire[97], B.M.M. Allbrooke[216], J.S. Allen[151], J.F. Allen[79], P.P. Allport[23], A. Aloisio[107,108], F. Alonso[140], C. Alpigiani[204], Z.M.K. Alsolami[141], A. Alvarez Fernandez[150], M. Alves Cardoso[83], M.G. Alviggi[107,108], M. Aly[151], Y. Amaral Coutinho[126], A. Ambler[154], C. Amelung[61], M. Amerl[151], C.G. Ames[159], D. Amidei[156], B. Amini[81], K. Amirie[227], A. Amirkhanov[64], S.P. Amor Dos Santos[184], K.R. Amos[236], D. Amperiadou[224], S. An[130], V. Ananiev[179], C. Anastopoulos[209], T. Andeen[12], J.K. Anders[142], A.C. Anderson[87], A. Andreazza[105,106], S. Angelidakis[10], A. Angerami[67], A.V. Anisenkov[64], A. Annovi[111], C. Antel[83], E. Antipov[215], M. Antonelli[80], F. Anulli[113], M. Aoki[130], T. Aoki[225], M.A. Aparo[216], L. Aperio Bella[75], C. Appelt[223], A. Apyan[33], S.J. Arbiol Val[136], C. Arcangeletti[80], A.T.H. Arce[78], J-F. Arguin[158], S. Argyropoulos[224], J.-H. Arling[75], O. Arnaez[5], H. Arnold[215], G. Artoni[113,114], H. Asada[161], K. Asai[172], S. Asai[225], N.A. Asbah[61], R.A. Ashby Pickering[240], A.M. Aslam[145], K. Assamagan[43], R. Astalos[41], K.S.V. Astrand[148], S. Atashi[232], R.J. Atkin[47], H. Atmani[60], P.A. Atmasiddha[182], K. Augsten[192], A.D. Auriol[66], V.A. Austrup[151], G. Avolio[61], K. Axiotis[83], G. Azuelos[158,281], D. Babal[42], H. Bachacou[195], K. Bachas[224,264], A. Bachiu[54], E. Bachmann[77], M.J. Backes[91], A. Badea[65], T.M. Baer[156], P. Bagnaia[113,114], M. Bahmani[21], D. Bahner[81], K. Bai[177], J.T. Baines[194], L. Baines[144], O.K. Baker[245], E. Bakos[17], D. Bakshi Gupta[9], L.E. Balabram Filho[126], V. Balakrishnan[174], R. Balasubramanian[5], E.M. Baldin[63], P. Balek[134], E. Ballabene[29,30], F. Balli[195], L.M. Baltes[91], W.K. Balunas[46], J. Balz[150], I. Bamwidhi[170], E. Banas[136], M. Bandieramonte[183], A. Bandyopadhyay[31], S. Bansal[31], L. Barak[223], M. Barakat[75], E.L. Barberio[155], D. Barberis[20], M. Barbero[152], M.Z. Barel[167], T. Barillari[160], M-S. Barisits[61], T. Barklow[213], P. Baron[176], D.A. Baron Moreno[151], A. Baroncelli[90], A.J. Barr[180], J.D. Barr[146], F. Barreiro[149], J. Barreiro Guimarães da Costa[15], M.G. Barros Teixeira[184], S. Barsov[63], F. Bartels[91], R. Bartoldus[213], A.E. Barton[141], P. Bartos[41], A. Basan[150], M. Baselga[76], S. Bashiri[136], A. Bassalat[97,248], M.J. Basso[228], S. Bataju[71], R. Bate[237], R.L. Bates[87], S. Batlamous[149], M. Battaglia[196], D. Battulga[21], M. Bauce[113,114], M. Bauer[121], P. Bauer[31], L.T. Bayer[75], L.T. Bazzano Hurrell[44], J.B. Beacham[160], T. Beau[181], J.Y. Beaucamp[140], P.H. Beauchemin[231], P. Bechtle[31], H.P. Beck[22,263], K. Becker[240], A.J. Beddall[124], V.A. Bednyakov[64], C.P. Bee[215], L.J. Beemster[17], M. Begalli[128], M. Begel[43], J.K. Behr[75], J.F. Beirer[61], F. Beisiegel[31], M. Belfkir[170], G. Bella[223], L. Bellagamba[30], A. Bellerive[54], P. Bellos[23], K. Beloborodov[63], D. Benchekroun[55], F. Bendebba[55], Y. Benhammou[223], K.C. Benkendorfer[89], L. Beresford[75], M. Beretta[80], E. Bergeaas Kuutmann[234], N. Berger[5], B. Bergmann[192], J. Beringer[19], G. Bernardi[6], C. Bernius[213], F.U. Bernlochner[31], F. Bernon[61], A. Berrocal Guardia[14], T. Berry[145], P. Berta[193], A. Berthold[77], R. Bertrand[152], S. Bethke[160], A. Betti[113,114], A.J. Bevan[144], L. Bezio[83], N.K. Bhalla[81], S. Bharthuar[160], S. Bhatta[215], D.S. Bhattacharya[239], P. Bhattarai[213], Z.M. Bhatti[171], K.D. Bhide[81], V.S. Bhopatkar[175], R.M. Bianchi[183], G. Bianco[29,30], O. Biebel[159], M. Biglietti[117], C.S. Billingsley[71], Y. Bimgdi[60], M. Bindi[82], A. Bingham[244], A. Bingul[25], C. Bini[113,114], G.A. Bird[46], M. Birman[242], M. Biros[193], S. Biryukov[216], T. Bisanz[76], E. Bisceglie[29,30], J.P. Biswal[194], D. Biswas[211], I. Bloch[75], A. Blue[87], U. Blumenschein[144], J. Blumenthal[150], V.S. Bobrovnikov[64], M. Boehler[81], B. Boehm[239], D. Bogavac[61], A.G. Bogdanchikov[63], L.S. Boggia[181], V. Boisvert[145], P. Bokan[61], T. Bold[134], M. Bomben[6], M. Bona[144], M. Boonekamp[195], A.G. Borbély[87], I.S. Bordulev[63], G. Borissov[141], D. Bortoletto[180], D. Boscherini[30], M. Bosman[14], K. Bouaouda[55], N. Bouchhar[236], L. Boudet[5], J. Boudreau[183], E.V. Bouhova-Thacker[141], D. Boumediene[66], R. Bouquet[85,84], A. Boveia[173], J. Boyd[61], D. Boye[43], I.R. Boyko[64], L. Bozianu[83], J. Bracinik[23], N. Brahimi[5], G. Brandt[244], O. Brandt[46], B. Brau[153], J.E. Brau[177], R. Brener[242], L. Brenner[167], R. Brenner[234], S. Bressler[242], G. Brianti[119,120], D. Britton[87], D. Britzger[160], I. Brock[31], R. Brock[157], G. Brooijmans[67], A.J. Brooks[99], E.M. Brooks[229], E. Brost[43], L.M. Brown[228,238], L.E. Bruce[89], T.L. Bruckler[180], P.A. Bruckman de Renstrom[136], B. Brüers[75], A. Bruni[30], G. Bruni[30], D. Brunner[73,74], M. Bruschi[30], N. Bruscino[113,114], T. Buanes[18], Q. Buat[204], D. Buchin[160], A.G. Buckley[87], O. Bulekov[63], B.A. Bullard[213], S. Burdin[142], C.D.

Burgard[76], A.M. Burger[61], B. Burghgrave[9], O. Burlayenko[81], J. Burleson[235], J.T.P. Burr[46], J.C. Burzynski[212], E.L. Busch[67], V. Büscher[150], P.J. Bussey[87], J.M. Butler[32], C.M. Buttar[87], J.M. Butterworth[146], W. Buttinger[194], C.J. Buxo Vazquez[157], A.R. Buzykaev[64], S. Cabrera Urbán[236], L. Cadamuro[97], D. Caforio[86], H. Cai[183], Y. Cai[164,29,30], Y. Cai[162], V.M.M. Cairo[61], O. Cakir[3], N. Calace[61], P. Calafiura[19], G. Calderini[181], P. Calfayan[54], G. Callea[87], L.P. Caloba[126], D. Calvet[66], S. Calvet[66], R. Camacho Toro[181], S. Camarda[61], D. Camarero Munoz[33], P. Camarri[115,116], M.T. Camerlingo[107,108], C. Camincher[238], M. Campanelli[146], A. Camplani[68], V. Canale[107,108], A.C. Canbay[3], E. Canonero[145], J. Cantero[236], Y. Cao[235], F. Capocasa[33], M. Capua[70,69], A. Carbone[105,106], R. Cardarelli[115], J.C.J. Cardenas[9], M.P. Cardiff[33], G. Carducci[70,69], T. Carli[61], G. Carlino[107], J.I. Carlotto[14], B.T. Carlson[183,265], E.M. Carlson[238], J. Carmignani[142], L. Carminati[105,106], A. Carnelli[5], M. Carnesale[61], S. Caron[166], E. Carquin[202], I.B. Carr[155], S. Carrá[105], G. Carratta[29,30], A.M. Carroll[177], M.P. Casado[14,255], M. Caspar[75], F.L. Castillo[5], L. Castillo Garcia[14], V. Castillo Gimenez[236], N.F. Castro[188,184], A. Catinaccio[61], J.R. Catmore[179], T. Cavaliere[5], V. Cavaliere[43], L.J. Caviedes Betancourt[28], Y.C. Cekmecelioglu[75], E. Celebi[124], S. Cella[61], V. Cepaitis[83], K. Cerny[176], A.S. Cerqueira[125], A. Cerri[111,285], L. Cerrito[115,116], F. Cerutti[19], B. Cervato[105,106], A. Cervelli[30], G. Cesarini[80], S.A. Cetin[124], P.M. Chabrillat[181], J. Chan[19], W.Y. Chan[225], J.D. Chapman[46], E. Chapon[195], B. Chargeishvili[220], D.G. Charlton[23], C. Chauhan[193], Y. Che[162], S. Chekanov[7], S.V. Chekulaev[228], G.A. Chelkov[64,247], B. Chen[223], B. Chen[238], H. Chen[162], H. Chen[43], J. Chen[207], J. Chen[212], M. Chen[180], S. Chen[137], S.J. Chen[162], X. Chen[207], X. Chen[16,280], Z. Chen[90], C.L. Cheng[243], H.C. Cheng[93], S. Cheong[213], A. Cheplakov[64], E. Cheremushkina[75], E. Cherepanova[167], R. Cherkaoui El Moursli[59], E. Cheu[8], K. Cheung[96], L. Chevalier[195], V. Chiarella[80], G. Chiarelli[111], N. Chiedde[152], G. Chiodini[103], A.S. Chisholm[23], A. Chitan[35], M. Chitishvili[236], M.V. Chizhov[64,266], K. Choi[12], Y. Chou[204], E.Y.S. Chow[166], K.L. Chu[242], M.C. Chu[93], X. Chu[15,164], Z. Chubinidze[80], J. Chudoba[191], J.J. Chwastowski[136], D. Cieri[160], K.M. Ciesla[134], V. Cindro[143], A. Ciocio[19], F. Cirotto[107,108], Z.H. Citron[242], M. Citterio[105], D.A. Ciubotaru[35], A. Clark[83], P.J. Clark[79], N. Clarke Hall[146], C. Clarry[227], S.E. Clawson[75], C. Clement[73,74], Y. Coadou[152], M. Cobal[100,102], A. Coccaro[85], R.F. Coelho Barrue[184], R. Coelho Lopes De Sa[153], S. Coelli[105], L.S. Colangeli[227], B. Cole[67], P. Collado Soto[149], J. Collot[88], P. Conde Muiño[184,190], M.P. Connell[49], S.H. Connell[49], E.I. Conroy[180], M. Contreras Cossio[12], F. Conventi[107,282], H.G. Cooke[23], A.M. Cooper-Sarkar[180], L. Corazzina[113,114], F.A. Corchia[29,30], A. Cordeiro Oudot Choi[181], L.D. Corpe[66], M. Corradi[113,114], F. Corriveau[154,274], A. Cortes-Gonzalez[21], M.J. Costa[236], F. Costanza[5], D. Costanzo[209], B.M. Cote[173], J. Couthures[5], G. Cowan[145], K. Cranmer[243], L. Cremer[76], D. Cremonini[29,30], S. Crépé-Renaudin[88], F. Crescioli[181], T. Cresta[109,110], M. Cristinziani[211], M. Cristoforetti[119,120], V. Croft[167], J.E. Crosby[175], G. Crosetti[70,69], A. Cueto[149], H. Cui[146], Z. Cui[8], W.R. Cunningham[87], F. Curcio[236], J.R. Curran[79], P. Czodrowski[61], M.J. Da Cunha Sargedas De Sousa[85,84], J.V. Da Fonseca Pinto[126], C. Da Via[151], W. Dabrowski[134], T. Dado[61], S. Dahbi[218], T. Dai[156], D. Dal Santo[22], C. Dallapiccola[153], M. Dam[68], G. D'amen[43], V. D'Amico[159], J. Damp[150], J.R. Dandoy[54], D. Dannheim[61], M. Danninger[212], V. Dao[215], G. Darbo[85], S.J. Das[43], F. Dattola[75], S. D'Auria[105,106], A. D'Avanzo[107,108], T. Davidek[193], J. Davidson[240], I. Dawson[144], H.A. Day-hall[192], K. De[9], C. De Almeida Rossi[227], R. De Asmundis[107], N. De Biase[75], S. De Castro[29,30], N. De Groot[166], P. de Jong[167], H. De la Torre[168], A. De Maria[162], A. De Salvo[113], U. De Sanctis[115,116], F. De Santis[103,104], A. De Santo[216], J.B. De Vivie De Regie[88], J. Debevc[143], D.V. Dedovich[64], J. Degens[142], A.M. Deiana[71], J. Del Peso[149], L. Delagrange[181], F. Deliot[195], C.M. Delitzsch[76], M. Della Pietra[107,108], D. Della Volpe[83], A. Dell'Acqua[61], L. Dell'Asta[105,106], M. Delmastro[5], C.C. Delogu[150], P.A. Delsart[88], S. Demers[245], M. Demichev[64], S.P. Denisov[63], H. Denizli[24,258], L. D'Eramo[66], D. Derendarz[136], F. Derue[181], P. Dervan[142,289], K. Desch[31], C. Deutsch[31], F.A. Di Bello[85,84], A. Di Ciaccio[115,116], L. Di Ciaccio[5], A. Di Domenico[113,114], C. Di Donato[107,108], A. Di Girolamo[61], G. Di Gregorio[61], A. Di Luca[119,120], B. Di Micco[117,118], R. Di Nardo[117,118], K.F. Di Petrillo[65], M. Diamantopoulou[54], F.A. Dias[167], T. Dias Do Vale[212], M.A. Diaz[197,198], A.R. Didenko[64], M. Didenko[236], E.B. Diehl[156], S. Díez Cornell[75], C. Diez Pardos[211], C. Dimitriadi[214], A. Dimitrievska[23], A. Dimri[215], J. Dingfelder[31], T. Dingley[180], I-M. Dinu[35], S.J. Dittmeier[92], F. Dittus[61], M. Divisek[193], B. Dixit[142], F. Djama[152], T. Djobava[220], C. Doglioni[148,151], A. Dohnalova[41], Z. Dolezal[193], K. Domijan[134], K.M. Dona[65], M. Donadelli[128], B. Dong[157], J. Donini[66], A. D'Onofrio[107,108], M. D'Onofrio[142], J. Dopke[194], A. Doria[107], N. Dos Santos Fernandes[184], P. Dougan[151], M.T. Dova[140], A.T. Doyle[87], M.A. Draguet[180], M.P. Drescher[82], E. Dreyer[242], I. Drivas-koulouris[11], M. Drnevich[171], M. Drozdova[83], D. Du[90], T.A. du Pree[167], F. Dubinin[64], M. Dubovsky[41], E. Duchovni[242], G. Duckeck[159], P.K. Duckett[146], O.A. Ducu[35], D. Duda[79], A. Dudarev[61], E.R. Duden[33], M. D'uffizi[151], L. Duflot[97], M. Dührssen[61], I. Duminica[40], A.E. Dumitriu[35], M. Dunford[91], S. Dungs[76], K. Dunne[73,74], A. Duperrin[152], H. Duran Yildiz[3], M. Düren[86], A. Durglishvili[220], D. Duvnjak[54], B.L. Dwyer[168], G.I. Dyckes[19], M. Dyndal[134], B.S. Dziedzic[61], Z.O. Earnshaw[216], G.H. Eberwein[180], B. Eckerova[41], S. Eggebrecht[82], E. Egidio Purcino De Souza[129], G. Eigen[18], K. Einsweiler[19], T. Ekelof[234], P.A. Ekman[148], S. El Farkh[56], Y. El Ghazali[90], H. El Jarrari[61], A. El Moussaouy[55], V. Ellajosyula[234], M. Ellert[234], F. Ellinghaus[244], N. Ellis[61], J. Elmsheuser[43], M. Elsawy[169], M. Elsing[61], D. Emeliyanov[194], Y. Enari[130], I. Ene[19], S. Epari[158], D. Ernani Martins Neto[136], M. Errenst[244], M. Escalier[97], C. Escobar[236], E. Etzion[223], G. Evans[185,184], H. Evans[99], L.S. Evans[145], A. Ezhilov[63], S. Ezzarqtouni[55], F. Fabbri[29,30], L. Fabbri[29,30], G. Facini[146], V. Fadeyev[196], R.M. Fakhrutdinov[63], D. Fakoudis[150], S. Falciano[113], L.F. Falda Ulhoa Coelho[184], F. Fallavollita[160], G. Falsetti[70,69], J. Faltova[193], C. Fan[235], K.Y. Fan[94], Y. Fan[15], Y. Fang[15,164], M. Fanti[105,106], M. Faraj[100,101], Z. Farazpay[147], A. Farbin[9], A. Farilla[117], T. Farooque[157], J.N. Farr[245], S.M. Farrington[79,194], F. Fassi[59], D. Fassouliotis[10], L. Fayard[97], P. Federic[193], P. Federicova[191], O.L. Fedin[63,247], M. Feickert[243], L. Feligioni[152], D.E. Fellers[19], C. Feng[205], Z. Feng[167], M.J. Fenton[232], L. Ferencz[75], B. Fernandez Barbadillo[141], P. Fernandez Martinez[98], M.J.V. Fernoux[152], J. Ferrando[141], A. Ferrari[234], P. Ferrari[167,166], R. Ferrari[109], D. Ferrere[83], C. Ferretti[156], M.P. Fewell[1], D. Fiacco[113,114], F. Fiedler[150], P. Fiedler[192], S. Filimonov[64], A. Filipčič[143], E.K. Filmer[228], F. Filthaut[166], M.C.N. Fiolhais[184,186,249], L. Fiorini[236], W.C. Fisher[157], T. Fitschen[151], P.M. Fitzhugh[195], I. Fleck[211], P. Fleischmann[156], T. Flick[244], M. Flores[50,278], L.R. Flores Castillo[93], L. Flores Sanz De Acedo[61], F.M. Follega[119,120], N. Fomin[46], J.H. Foo[227], A. Formica[195], A.C. Forti[151], E. Fortin[61], A.W. Fortman[19], L. Fountas[10,256], D. Fournier[97], H. Fox[141], P. Francavilla[111,112], S. Francescato[89], S. Franchellucci[83], M. Franchini[29,30], S. Franchino[91], D. Francis[61], L. Franco[166], V. Franco Lima[61], L. Franconi[75], M. Franklin[89], G. Frattari[33], Y.Y. Frid[223], J. Friend[87], N. Fritzsche[61], A. Froch[83], D. Froidevaux[61], J.A. Frost[180], Y. Fu[157], S. Fuenzalida Garrido[202], M. Fujimoto[152], K.Y. Fung[93], E. Furtado De Simas Filho[129], M. Furukawa[225], J. Fuster[236], A. Gaa[82], A. Gabrielli[29,30], A. Gabrielli[227], P. Gadow[61], G. Gagliardi[85,84], L.G. Gagnon[19], S. Gaid[132], S. Galantzan[223], J. Gallagher[1], E.J. Gallas[180], A.L. Gallen[234], B.J. Gallop[194], K.K. Gan[173], S. Ganguly[225], Y. Gao[79], A. Garabaglu[204], F.M. Garay Walls[197,198], B. Garcia[43], C. García[236], A. Garcia Alonso[167], A.G. Garcia Caffaro[245], J.E. García Navarro[236], M. Garcia-Sciveres[19], G.L. Gardner[182], R.W.

Gardner[65], N. Garelli[231], R.B. Garg[213], J.M. Gargan[79], C.A. Garner[227], C.M. Garvey[47], V.K. Gassmann[231], G. Gaudio[109], V. Gautam[14], P. Gauzzi[113,114], J. Gavranovic[143], I.L. Gavrilenko[184], A. Gavrilyuk[63], C. Gay[237], G. Gaycken[177], E.N. Gazis[11], A. Gekow[173], C. Gemme[85], M.H. Genest[88], A.D. Gentry[165], S. George[145], W.F. George[23], T. Geralis[72], A.A. Gerwin[174], P. Gessinger-Befurt[61], M.E. Geyik[244], M. Ghani[240], K. Ghorbanian[144], A. Ghosal[211], A. Ghosh[232], A. Ghosh[8], B. Giacobbe[30], S. Giagu[113,114], T. Giani[167], A. Giannini[90], S.M. Gibson[145], M. Gignac[196], D.T. Gil[135], A.K. Gilbert[134], B.J. Gilbert[67], D. Gillberg[54], G. Gilles[167], L. Ginabat[181], D.M. Gingrich[2,281], M.P. Giordani[100,102], P.F. Giraud[195], G. Giugliarelli[100,102], D. Giugni[105], F. Giuli[115,116], I. Gkialas[10,256], L.K. Gladilin[63], C. Glasman[149], G. Glemža[75], M. Glisic[177], I. Gnesi[70], Y. Go[43], M. Goblirsch-Kolb[61], B. Gocke[76], D. Godin[158], B. Gokturk[24], S. Goldfarb[155], T. Golling[83], M.G.D. Gololo[49], D. Golubkov[63], J.P. Gombas[157], A. Gomes[184,185], G. Gomes Da Silva[211], A.J. Gomez Delegido[236], R. Gonçalo[184], L. Gonella[23], A. Gongadze[221], F. Gonnella[23], J.L. Gonski[213], R.Y. González Andana[79], S. González de la Hoz[236], C. Gonzalez Renteria[19], M.V. Gonzalez Rodrigues[75], R. Gonzalez Suarez[234], S. Gonzalez-Sevilla[83], L. Goossens[61], B. Gorini[61], E. Gorini[103,104], A. Gorišek[143], T.C. Gosart[182], A.T. Goshaw[78], M.I. Gostkin[64], S. Goswami[175], C.A. Gottardo[61], S.A. Gotz[159], M. Gouighri[56], A.G. Goussiou[204], N. Govender[49], R.P. Grabarczyk[180], I. Grabowska-Bold[134], K. Graham[54], E. Gramstad[179], S. Grancagnolo[103,104], C.M. Grant[1,195], P.M. Gravila[39], F.G. Gravili[103,104], H.M. Gray[19], M. Greco[160], M.J. Green[1], C. Grefe[31], A.S. Grefsrud[18], I.M. Gregor[75], K.T. Greif[232], P. Grenier[213], S.G. Grewe[160], A.A. Grillo[196], K. Grimm[45], S. Grinstein[14,270], J.-F. Grivaz[97], E. Gross[242], J. Grosse-Knetter[82], L. Guan[156], G. Guerrieri[61], R. Guevara[179], R. Gugel[150], J.A.M. Guhit[156], A. Guida[21], E. Guilloton[240], S. Guindon[61], F. Guo[15,164], J. Guo[207], L. Guo[75], L. Guo[163,268], Y. Guo[156], A. Gupta[76], R. Gupta[183], S. Gurbuz[31], S.S. Gurdasani[75], G. Gustavino[113,114], P. Gutierrez[174], L.F. Gutierrez Zagazeta[182], M. Gutsche[77], C. Gutschow[146], C. Gwenlan[180], C.B. Gwilliam[142], E.S. Haaland[179], A. Haas[171], M. Habedank[87], C. Haber[19], H.K. Hadavand[9], A. Haddad[66], A. Hadef[77], A.I. Hagan[141], J.J. Hahn[211], E.H. Haines[146], M. Haleem[239], J. Haley[175], G.D. Hallewell[152], L. Halser[22], K. Hamano[238], M. Hamer[31], S.E.D. Hammoud[97], E.J. Hampshire[145], J. Han[205], L. Han[162], L. Han[90], S. Han[19], K. Hanagaki[130], M. Hance[196], D.A. Hangal[67], H. Hanif[212], M.D. Hank[182], J.B. Hansen[68], P.H. Hansen[68], D. Harada[83], T. Harenberg[244], S. Harkusha[246], M.L. Harris[153], Y.T. Harris[31], J. Harrison[14], N.M. Harrison[173], P.F. Harrison[240], M.L.E. Hart[146], N.M. Hartman[160], N.M. Hartmann[159], R.Z. Hasan[145,194], Y. Hasegawa[210], F. Haslbeck[180], S. Hassan[18], R. Hauser[157], M. Haviernik[193], C.M. Hawkes[23], R.J. Hawkings[61], Y. Hayashi[225], D. Hayden[157], C. Hayes[156], R.L. Hayes[167], C.P. Hays[180], J.M. Hays[144], H.S. Hayward[142], F. He[90], M. He[15,164], Y. He[75], Y. He[146], N.B. Heatley[144], V. Hedberg[148], A.L. Heggelund[179], C. Heidegger[81], K.K. Heidegger[81], J. Heilman[54], S. Heim[75], T. Heim[19], J.G. Heinlein[182], J.J. Heinrich[177], L. Heinrich[160,279], J. Hejbal[191], A. Held[243], S. Hellesund[18], C.M. Helling[237], S. Hellman[73,74], L. Henkelmann[46], A.M. Henriques Correia[61], H. Herde[148], Y. Hernández Jiménez[215], L.M. Herrmann[31], T. Herrmann[77], G. Herten[81], R. Hertenberger[159], L. Hervas[61], M.E. Hesping[150], N.P. Hessey[228], J. Hessler[160], M. Hidaoui[56], N. Hidic[193], E. Hill[227], S.J. Hillier[23], J.R. Hinds[157], F. Hinterkeuser[31], M. Hirose[178], S. Hirose[230], D. Hirschbuehl[244], T.G. Hitchings[151], B. Hiti[143], J. Hobbs[215], R. Hobincu[38], N. Hod[242], M.C. Hodgkinson[209], B.H. Hodkinson[180], A. Hoecker[61], D.D. Hofer[156], J. Hofer[236], M. Holzbock[61], L.B.A.H. Hommels[46], V. Homsak[180], B.P. Honan[151], J.J. Hong[99], J. Hong[207], T.M. Hong[183], B.H. Hooberman[235], W.H. Hopkins[7], M.C. Hoppesch[235], Y. Horii[161], M.E. Horstmann[160], S. Hou[218], M.R. Housenga[235], A.S. Howard[143], J. Howarth[87], J. Hoya[7], M. Hrabovsky[176], T. Hryn'ova[5], P.J. Hsu[96], S.-C. Hsu[204], T. Hsu[97], M. Hu[19], Q. Hu[90], S. Huang[46], X. Huang[15,164], Y. Huang[193], Y. Huang[163], Y. Huang[150], Y. Huang[15], Z. Huang[151], Z. Hubacek[192], M. Huebner[31], F. Huegging[31], T.B. Huffman[180], M. Hufnagel Maranha De Faria[125], C.A. Hugli[75], M. Huhtinen[61], S.K. Huiberts[18], R. Hulsken[154], C.E. Hultquist[19], N. Huseynov[13,253], J. Huston[157], J. Huth[89], R. Hyneman[8], G. Iacobucci[83], G. Iakovidis[43], L. Iconomidou-Fayard[97], J.P. Iddon[61], P. Iengo[107,108], R. Iguchi[225], Y. Iiyama[225], T. Iizawa[180], Y. Ikegami[130], D. Iliadis[224], N. Ilic[227], H. Imam[127], G. Inacio Goncalves[128], S.A. Infante Cabanas[199], T. Ingebretsen Carlson[73,74], J.M. Inglis[144], G. Introzzi[109,110], M. Iodice[117], V. Ippolito[113,114], R.K. Irwin[142], M. Ishino[225], W. Islam[243], C. Issever[21], S. Istin[24,288], K. Itabashi[130], H. Ito[241], R. Iuppa[119,120], A. Ivina[242], V. Izzo[107], P. Jacka[191], P. Jackson[1], P. Jain[75], K. Jakobs[81], T. Jakoubek[242], J. Jamieson[87], W. Jang[225], S. Jankovych[193], M. Javurkova[153], P. Jawahar[151], L. Jeanty[177], J. Jejelava[219,277], P. Jenni[81,252], C.E. Jessiman[54], C. Jia[205], H. Jia[237], J. Jia[215], X. Jia[15,164], Z. Jia[162], C. Jiang[79], Q. Jiang[94], S. Jiggins[75], M. Jimenez Ortega[236], J. Jimenez Pena[14], S. Jin[162], A. Jinaru[35], O. Jinnouchi[203], P. Johansson[209], K.A. Johns[8], J.W. Johnson[196], F.A. Jolly[75], D.M. Jones[216], E. Jones[75], K.S. Jones[9], P. Jones[46], R.W.L. Jones[141], T.J. Jones[142], H.L. Joos[61,82], R. Joshi[173], J. Jovicevic[17], X. Ju[19], J.J. Junggeburth[61], T. Junkermann[91], A. Juste Rozas[14,270], M.K. Juzek[136], S. Kabana[201], A. Kaczmarska[136], M. Kado[160], H. Kagan[173], M. Kagan[213], A. Kahn[182], C. Kahra[150], T. Kaji[225], E. Kajomovitz[222], N. Kakati[242], N. Kakoty[14], I. Kalaitzidou[81], S. Kandel[9], N.J. Kang[196], D. Kar[53,289], K. Karava[180], E. Karentzos[31], O. Karkout[167], S.N. Karpov[64], Z.M. Karpova[64], V. Kartvelishvili[141], A.N. Karyukhin[63], E. Kasimi[224], J. Katzy[75], S. Kaur[54], K. Kawade[210], M.P. Kawale[174], C. Kawamoto[137], T. Kawamoto[90], E.F. Kay[61], F.I. Kaya[231], S. Kazakos[157], V.F. Kazanin[63], Y. Ke[215], J.M. Keaveney[47], R. Keeler[238], G.V. Kehris[89], J.S. Keller[54], J.J. Kempster[216], O. Kepka[191], J. Kerr[229], B.P. Kerridge[194], B.P. Kerševan[143], L. Keszeghova[41], R.A. Khan[183], A. Khanov[175], A.G. Kharlamov[63], T. Kharlamova[63], E.E. Khoda[204], M. Kholodenko[184], T.J. Khoo[21], G. Khoriauli[239], J. Khubua[220,289], Y.A.R. Khwaira[181], B. Kibirige[53], D. Kim[7], D.W. Kim[73,74], Y.K. Kim[65], N. Kimura[146], M.K. Kingston[82], A. Kirchhoff[82], C. Kirfel[31], F. Kirfel[31], J. Kirk[194], A.E. Kiryunin[160], S. Kita[230], C. Kitsaki[11], O. Kivernyk[31], M. Klassen[231], C. Klein[54], L. Klein[239], M.H. Klein[71], S.B. Klein[83], U. Klein[142], A. Klimentov[43], T. Klioutchnikova[61], P. Kluit[167], S. Kluth[160], E. Kneringer[121], T.M. Knight[227], A. Knue[76], M. Kobel[77], D. Kobylianskii[242], S.F. Koch[180], M. Kocian[213], P. Kodyš[193], D.M. Koeck[177], P.T. Koenig[31], T. Koffas[54], O. Kolay[77], I. Koletsou[5], T. Komarek[136], K. Köneke[82], A.X.Y. Kong[1], T. Kono[172], N. Konstantinidis[146], P. Kontaxakis[83], B. Konya[148], R. Kopeliansky[67], S. Koperny[134], K. Korcyl[136], K. Kordas[224,251], A. Korn[146], S. Korn[82], I. Korolkov[14], N. Korotkova[63], B. Kortman[167], O. Kortner[160], S. Kortner[160], W.H. Kostecka[168], M. Kostov[41], V.V. Kostyukhin[211], A. Kotsokechagia[61], A. Kotwal[78], A. Koulouris[61], A. Kourkoumeli-Charalampidi[109,110], C. Kourkoumelis[10], E. Kourlitis[160], O. Kovanda[177], R. Kowalewski[238], W. Kozanecki[177], A.S. Kozhin[63], V.A. Kramarenko[63], G. Kramberger[143], P. Kramer[31], M.W. Krasny[181], A. Krasznahorkay[153], A.C. Kraus[168], J.W. Kraus[244], J.A. Kremer[75], N.B. Krengel[211], T. Kresse[77], L. Kretschmann[244], J. Kretzschmar[142], K. Kreul[21], P. Krieger[227], K. Krizka[23], K. Kroeninger[76], H. Kroha[160], J. Kroll[191], J. Kroll[182], K.S. Krowpman[157], U. Kruchonak[64], H. Krüger[31], N. Krumnack[123], M.C. Kruse[78], O. Kuchinskaia[64], S. Kuday[3], S. Kuehn[61], R. Kuesters[81], T. Kuhl[75], V. Kukhtin[64], Y. Kulchitsky[64], S. Kuleshov[200,198], M. Kumar[53], N. Kumari[75], P. Kumari[229], A. Kupco[191], T. Kupfer[76], A. Kupich[63], O. Kuprash[81], H. Kurashige[133], L.L. Kurchaninov[228], O. Kurdysh[5], Y.A. Kurochkin[62], A. Kurova[63], M. Kuze[203], A.K. Kvam[153], J. Kvita[176], N.G. Kyriacou[156], L.A.O. Laatu[152], C.

Lacasta[236], F. Lacava[113,114], H. Lacker[21], D. Lacour[181], N.N. Lad[146], E. Ladygin[64], A. Lafarge[66], B. Laforge[181], T. Lagouri[245], F.Z. Lahbabi[55], S. Lai[82], J.E. Lambert[238], S. Lammers[99], W. Lampl[8], C. Lampoudis[224,251], G. Lamprinoudis[150], A.N. Lancaster[168], E. Lançon[43], U. Landgraf[81], M.P.J. Landon[144], V.S. Lang[81], O.K.B. Langrekken[179], A.J. Lankford[232], F. Lanni[61], K. Lantzsch[31], A. Lanza[109], M. Lanzac Berrocal[236], J.F. Laporte[195], T. Lari[105], D. Larsen[18], F. Lasagni Manghi[30], M. Lassnig[61], V. Latonova[191], S.D. Lawlor[209], Z. Lawrence[151], R. Lazaridou[240], M. Lazzaroni[105,106], H.D.M. Le[157], E.M. Le Boulicaut[245], L.T. Le Pottier[19], B. Leban[29,30], M. LeBlanc[151], F. Ledroit-Guillon[88], S.C. Lee[218], T.F. Lee[142], L.L. Leeuw[49,286], M. Lefebvre[238], C. Leggett[19], G. Lehmann Miotto[61], M. Leigh[83], W.A. Leight[153], W. Leinonen[166], A. Leisos[224,267], M.A.L. Leite[127], C.E. Leitgeb[21], R. Leitner[193], K.J.C. Leney[71], T. Lenz[31], S. Leone[111], C. Leonidopoulos[79], A. Leopold[214], J. LePage-Bourbonnais[54], R. Les[157], C.G. Lester[46], M. Levchenko[63], J. Levêque[5], L.J. Levinson[242], G. Levrini[29,30], M.P. Lewicki[136], C. Lewis[204], D.J. Lewis[5], L. Lewitt[209], A. Li[43], B. Li[205], C. Li[156], C-Q. Li[160], H. Li[90], H. Li[205], H. Li[151], H. Li[16], H. Li[90], H. Li[205], J. Li[207], K. Li[15], L. Li[207], R. Li[245], S. Li[15,164], S. Li[208,207,250], T. Li[6], X. Li[154], Z. Li[225], Z. Li[15,164], Z. Li[90], S. Liang[15,164], Z. Liang[15], M. Liberatore[195], B. Liberti[115], K. Lie[95], J. Lieber Marin[129], H. Lien[99], H. Lin[156], S.F. Lin[215], L. Linden[159], R.E. Lindley[8], J.H. Lindon[2], J. Ling[89], E. Lipeles[182], A. Lipniacka[18], A. Lister[237], J.D. Little[99], B. Liu[15], B.X. Liu[163], D. Liu[208,207], E.H.L. Liu[23], J.K.K. Liu[46], K. Liu[208], K. Liu[208,207], M. Liu[90], M.Y. Liu[90], P. Liu[15], Q. Liu[208,204,207], X. Liu[90], X. Liu[205], Y. Liu[163,164], Y.L. Liu[205], Y.W. Liu[90], Z. Liu[97,90], S.L. Lloyd[144], E.M. Lobodzinska[75], P. Loch[8], E. Lodhi[227], T. Lohse[21], K. Lohwasser[209], E. Loiacono[75], J.D. Lomas[23], J.D. Long[67], I. Longarini[232], R. Longo[235], A. Lopez Solis[75], N.A. Lopez-canelas[8], N. Lorenzo Martinez[5], A.M. Lory[159], M. Losada[169], G. Löschcke Centeno[216], O. Loseva[63], X. Lou[73,74], X. Lou[15,164], A. Lounis[97], P.A. Love[141], G. Lu[15,164], M. Lu[97], S. Lu[182], Y.J. Lu[218], H.J. Lubatti[204], C. Luci[113,114], F.L. Lucio Alves[162], F. Luehring[99], B.S. Lunday[182], O. Lundberg[214], B. Lund-Jensen[214,289], N.A. Luongo[7], M.S. Lutz[61], A.B. Lux[32], D. Lynn[43], R. Lysak[191], V. Lysenko[192], E. Lytken[148], V. Lyubushkin[64], T. Lyubushkina[64], M.M. Lyukova[215], H. Ma[43], K. Ma[90], L.L. Ma[205], W. Ma[90], Y. Ma[175], J.C. MacDonald[150], P.C. Machado De Abreu Farias[129], R. Madar[66], T. Madula[146], J. Maeda[133], T. Maeno[43], P.T. Mafa[49,257], H. Maguire[209], V. Maiboroda[97], A. Maio[184,185,187], K. Maj[134], O. Majersky[75], S. Majewski[177], R. Makhmanazarov[63], N. Makovec[97], V. Maksimovic[17], B. Malaescu[181], J. Malamant[179], Pa. Malecki[136], V.P. Maleev[63], F. Malek[88,262], M. Mali[143], D. Malito[145], U. Mallik[122,289], S. Maltezos[11], A. Malvezzi Lopes[128], S. Malyukov[64], J. Mamuzic[14], G. Mancini[80], M.N. Mancini[33], G. Manco[109,110], J.P. Mandalia[144], S.S. Mandarry[216], I. Mandić[143], L. Manhaes de Andrade Filho[125], I.M. Maniatis[242], J. Manjarres Ramos[139], D.C. Mankad[242], A. Mann[159], T. Manoussos[61], M.N. Mantinan[65], S. Manzoni[61], L. Mao[207], X. Mapekula[49], A. Marantis[224,267], R.R. Marcelo Gregorio[144], G. Marchiori[6], M. Marcisovsky[191], C. Marcon[105], M. Marinescu[23], S. Marium[75], M. Marjanovic[174], A. Markhoos[81], M. Markovitch[97], M.K. Maroun[153], G.T. Marsden[151], E.J. Marshall[141], Z. Marshall[19], S. Marti-Garcia[236], J. Martin[146], T.A. Martin[194], V.J. Martin[79], B. Martin dit Latour[18], L. Martinelli[113,114], M. Martinez[14,270], P. Martinez Agullo[236], V.I. Martinez Outschoorn[153], P. Martinez Suarez[14], S. Martin-Haugh[194], G. Martinovicova[193], V.S. Martoiu[35], A.C. Martyniuk[146], A. Marzin[61], D. Mascione[119,120], L. Masetti[150], J. Masik[151], A.L. Maslennikov[64], S.L. Mason[67], P. Massarotti[107,108], P. Mastrandrea[111,112], A. Mastroberardino[70,69], T. Masubuchi[178], T.T. Mathew[177], J. Matousek[193], D.M. Mattern[76], J. Maurer[35], T. Maurin[87], A.J. Maury[97], B. Maček[143], D.A. Maximov[63], A.E. May[151], E. Mayer[66], R. Mazini[53], I. Maznas[168], M. Mazza[157], S.M. Mazza[196], E. Mazzeo[105,106], J.P. Mc Gowan[238], S.P. Mc Kee[156], C.A. Mc Lean[7], C.C. McCracken[237], E.F. McDonald[155], A.E. McDougall[167], L.F. Mcelhinney[141], J.A. Mcfayden[216], R.P. McGovern[182], R.P. Mckenzie[53], T.C. Mclachlan[75], D.J. Mclaughlin[146], S.J. McMahon[194], C.M. Mcpartland[142], R.A. McPherson[238,274], S. Mehlhase[159], A. Mehta[142], D. Melini[236], B.R. Mellado Garcia[53], A.H. Melo[82], F. Meloni[75], A.M. Mendes Jacques Da Costa[151], H.Y. Meng[227], L. Meng[141], S. Menke[160], M. Mentink[61], E. Meoni[70,69], G. Mercado[168], S. Merianos[224], C. Merlassino[100,102], C. Meroni[105,106], J. Metcalfe[7], A.S. Mete[7], E. Meuser[150], C. Meyer[99], J-P. Meyer[195], R.P. Middleton[194], M. Mihovilovic[97], L. Mijović[79], G. Mikenberg[242], M. Mikestikova[191], M. Mikuž[143], H. Mildner[150], A. Milic[61], D.W. Miller[65], E.H. Miller[213], L.S. Miller[54], A. Milov[242], D.A. Milstead[73,74], T. Min[162], A.A. Minaenko[63], I.A. Minashvili[220], A.I. Mincer[171], B. Mindur[134], M. Mineev[64], Y. Mino[137], L.M. Mir[14], M. Miralles Lopez[87], M. Mironova[19], M. Missio[166], A. Mitra[240], V.A. Mitsou[236], Y. Mitsumori[161], O. Miu[227], P.S. Miyagawa[144], T. Mkrtchyan[91], M. Mlinarevic[146], T. Mlinarevic[146], M. Mlynarikova[61], S. Mobius[22], P. Mogg[159], M.H. Mohamed Farook[165], A.F. Mohammed[15,164], S. Mohapatra[67], M.F. Mohd Soberi[79], S. Mohiuddin[175], G. Mokgatitswane[53], L. Moleri[242], U. Molinatti[180], B. Mondal[211], S. Mondal[192], K. Mönig[75], E. Monnier[152], L. Monsonis Romero[236], J. Montejo Berlingen[14], A. Montella[73,74], M. Montella[173], F. Montereali[117,118], F. Monticelli[140], S. Monzani[100,102], A. Morancho Tarda[68], N. Morange[97], A.L. Moreira De Carvalho[75], M. Moreno Llácer[236], C. Moreno Martinez[83], J.M. Moreno Perez[28], P. Morettini[85], S. Morgenstern[61], M. Morii[89], M. Morinaga[225], M. Moritsu[138], F. Morodei[113,114], P. Moschovakos[61], B. Moser[180], M. Mosidze[220], T. Moskalets[71], P. Moskvitina[166], J. Moss[45,259], P. Moszkowicz[134], A. Moussa[58], Y. Moyal[242], E.J.W. Moyse[153], O. Mtintsilana[53], S. Muanza[152], J. Mueller[183], G.A. Mullier[234], A.J. Mullin[46], J.J. Mullin[78], A.E. Mulski[89], D.P. Mungo[227], D. Munoz Perez[236], F.J. Munoz Sanchez[151], M. Murin[151], W.J. Murray[240,194], M. Muškinja[143], C. Mwewa[43], A.G. Myagkov[63,247], A.J. Myers[9], G. Myers[156], M. Myska[192], B.P. Nachman[19], K. Nagai[180], K. Nagano[130], R. Nagasaka[225], J.L. Nagle[43,284], E. Nagy[152], A.M. Nairz[61], Y. Nakahama[130], K. Nakamura[130], K. Nakkalil[6], H. Nanjo[178], E.A. Narayanan[71], Y. Narukawa[225], I. Naryshkin[63], L. Nasella[105,106], S. Nasri[170], C. Nass[31], G. Navarro[27], J. Navarro-Gonzalez[236], A. Nayaz[21], P.Y. Nechaeva[63], S. Nechaeva[29,30], F. Nechansky[191], L. Nedic[180], T.J. Neep[23], A. Negri[109,110], M. Negrini[30], C. Nellist[167], C. Nelson[154], K. Nelson[156], S. Nemecek[191], M. Nessi[61,254], M.S. Neubauer[235], J. Newell[142], P.R. Newman[23], Y.W.Y. Ng[235], B. Ngair[169], H.D.N. Nguyen[158], R.B. Nickerson[180], R. Nicolaidou[195], J. Nielsen[196], M. Niemeyer[82], J. Niermann[61], N. Nikiforou[61], V. Nikolaenko[63,247], I. Nikolic-Audit[181], P. Nilsson[43], I. Ninca[75], G. Ninio[223], A. Nisati[113], N. Nishu[2], R. Nisius[160], N. Nitika[100,102], J-E. Nitschke[77], E.K. Nkadimeng[53], T. Nobe[225], T. Nommensen[217], M.B. Norfolk[209], B.J. Norman[54], M. Noury[55], J. Novak[143], T. Novak[143], R. Novotny[165], L. Nozka[176], K. Ntekas[232], N.M.J. Nunes De Moura Junior[126], J. Ocariz[181], A. Ochi[133], I. Ochoa[184], S. Oerdek[75,271], J.T. Offermann[65], A. Ogrodnik[193], A. Oh[151], C.C. Ohm[214], H. Oide[130], R. Oishi[225], M.L. Ojeda[61], Y. Okumura[225], L.F. Oleiro Seabra[184], I. Oleksiyuk[83], S.A. Olivares Pino[200], G. Oliveira Correa[14], D. Oliveira Damazio[43], J.L. Oliver[232], Ö.O. Öncel[81], A.P. O'Neill[22], A. Onofre[184,188], P.U.E. Onyisi[12], M.J. Oreglia[65], D. Orestano[117,118], R. Orlandini[117,118], R.S. Orr[227], L.M. Osojnak[182], Y. Osumi[161], G. Otero y Garzon[44], H. Otono[138], G.J. Ottino[19], M. Ouchrif[58], F. Ould-Saada[179], T. Ovsiannikova[204], M. Owen[87], R.E. Owen[194], V.E. Ozcan[24], F. Ozturk[136], N. Ozturk[9], S. Ozturk[124], H.A. Pacey[180], K. Pachal[228], A. Pacheco Pages[14], C. Padilla Aranda[14], G. Padovano[113,114], S. Pagan Griso[19], G. Palacino[99], A. Palazzo[103,104], J. Pampel[31],

J. Pan[245], T. Pan[93], D.K. Panchal[12], C.E. Pandini[167], J.G. Panduro Vazquez[194], H.D. Pandya[1], H. Pang[195], P. Pani[75], G. Panizzo[100,102], L. Panwar[181], L. Paolozzi[83], S. Parajuli[235], A. Paramonov[7], C. Paraskevopoulos[80], D. Paredes Hernandez[94], A. Pareti[109,110], K.R. Park[67], T.H. Park[160], F. Parodi[85,84], J.A. Parsons[67], U. Parzefall[81], B. Pascual Dias[66], L. Pascual Dominguez[149], E. Pasqualucci[113], S. Passaggio[85], F. Pastore[145], P. Patel[136], U.M. Patel[78], J.R. Pater[151], T. Pauly[61], F. Pauwels[193], C.I. Pazos[231], M. Pedersen[179], R. Pedro[184], S.V. Peleganchuk[63], O. Penc[61], E.A. Pender[79], S. Peng[16], G.D. Penn[245], K.E. Penski[159], M. Penzin[63], B.S. Peralva[128], A.P. Pereira Peixoto[204], L. Pereira Sanchez[213], D.V. Perepelitsa[43,284], G. Perera[153], E. Perez Codina[228], M. Perganti[11], H. Pernegger[61], S. Perrella[113,114], O. Perrin[66], K. Peters[75], R.F.Y. Peters[151], B.A. Petersen[61], T.C. Petersen[68], E. Petit[152], V. Petousis[192], A.R. Petri[105,106], C. Petridou[224,251], T. Petru[193], A. Petrukhin[211], M. Pettee[19], A. Petukhov[124], K. Petukhova[61], R. Pezoa[202], L. Pezzotti[29,30], G. Pezzullo[245], L. Pfaffenbichler[61], A.J. Pfleger[61], T.M. Pham[243], T. Pham[155], P.W. Phillips[194], G. Piacquadio[215], E. Pianori[19], F. Piazza[177], R. Piegaia[44], D. Pietreanu[35], A.D. Pilkington[151], M. Pinamonti[100,102], J.L. Pinfold[2], B.C. Pinheiro Pereira[184], J. Pinol Bel[14], A.E. Pinto Pinoargote[181], L. Pintucci[100,102], K.M. Piper[216], A. Pirttikoski[83], D.A. Pizzi[54], L. Pizzimento[94], A. Plebani[46], M.-A. Pleier[43], V. Pleskot[193], E. Plotnikova[64], G. Poddar[144], R. Poettgen[148], L. Poggioli[181], S. Polacek[193], G. Polesello[109], A. Poley[212,228], A. Polini[30], C.S. Pollard[240], Z.B. Pollock[173], E. Pompa Pacchi[174], N.I. Pond[146], D. Ponomarenko[99], L. Pontecorvo[61], S. Popa[34], G.A. Popeneciu[37], A. Poreba[61], D.M. Portillo Quintero[228], S. Pospisil[192], M.A. Postill[209], P. Postolache[36], K. Potamianos[240], P.A. Potepa[134], I.N. Potrap[64], C.J. Potter[46], H. Potti[217], J. Poveda[236], M.E. Pozo Astigarraga[61], A. Prades Ibanez[115,116], J. Pretel[238], D. Price[151], M. Primavera[103], L. Primomo[100,102], M.A. Principe Martin[149], R. Privara[176], T. Procter[87], M.L. Proffitt[204], N. Proklova[182], K. Prokofiev[95], G. Proto[160], J. Proudfoot[7], M. Przybycien[134], W.W. Przygoda[135], A. Psallidas[72], J.E. Puddefoot[209], D. Pudzha[81], D. Pyatiizbyantseva[166], J. Qian[156], R. Qian[157], D. Qichen[151], Y. Qin[14], T. Qiu[79], A. Quadt[82], M. Queitsch-Maitland[151], G. Quetant[83], R.P. Quinn[237], G. Rabanal Bolanos[89], D. Rafanoharana[81], F. Raffaeli[115,116], F. Ragusa[105,106], J.L. Rainbolt[65], J.A. Raine[83], S. Rajagopalan[43], E. Ramakoti[64], L. Rambelli[85,84], I.A. Ramirez-Berend[54], K. Ran[75,164], D.S. Rankin[182], N.P. Rapheeha[53], H. Rasheed[35], V. Raskina[181], D.F. Rassloff[91], A. Rastogi[19], S. Rave[150], S. Ravera[85,84], B. Ravina[61], I. Ravinovich[242], M. Raymond[61], A.L. Read[179], N.P. Readioff[209], D.M. Rebuzzi[109,110], A.S. Reed[160], K. Reeves[33], J.A. Reidelsturz[244], D. Reikher[177], A. Rej[76], C. Rembser[61], H. Ren[90], M. Renda[35], F. Renner[75], A.G. Rennie[232], A.L. Rescia[75], S. Resconi[105], M. Ressegotti[85], S. Rettie[61], W.F. Rettie[54], J.G. Reyes Rivera[157], E. Reynolds[19], O.L. Rezanova[64], P. Reznicek[193], H. Riani[58], N. Ribaric[78], E. Ricci[119,120], R. Richter[160], S. Richter[73,74], E. Richter-Was[135], M. Ridel[181], S. Ridouani[58], P. Rieck[171], P. Riedler[61], E.M. Riefel[73,74], J.O. Rieger[167], M. Rijssenbeek[215], M. Rimoldi[61], L. Rinaldi[29,30], P. Rincke[82], G. Ripellino[234], I. Riu[14], J.C. Rivera Vergara[238], F. Rizatdinova[175], E. Rizvi[144], B.R. Roberts[19], S.S. Roberts[196], D. Robinson[46], M. Robles Manzano[150], A. Robson[87], A. Rocchi[115,116], C. Roda[111,112], S. Rodriguez Bosca[61], Y. Rodriguez Garcia[27], A.M. Rodríguez Vera[168], S. Roe[61], J.T. Roemer[61], O. Røhne[179], R.A. Rojas[61], C.P.A. Roland[181], J. Roloff[43], A. Romaniouk[121], E. Romano[109,110], M. Romano[30], A.C. Romero Hernandez[235], N. Rompotis[142], L. Roos[181], S. Rosati[113], B.J. Rosser[65], E. Rossi[180], E. Rossi[107,108], L.P. Rossi[89], L. Rossini[81], R. Rosten[173], M. Rotaru[35], R. Roth[61], B. Rottler[81], D. Rousseau[97], D. Rousso[75], S. Roy-Garand[227], A. Rozanov[152], Z.M.A. Rozario[87], Y. Rozen[222], A. Rubio Jimenez[236], V.H. Ruelas Rivera[21], T.A. Ruggeri[1], A. Ruggiero[180], A. Ruiz-Martinez[236], A. Rummler[61], Z. Rurikova[81], N.A. Rusakovich[64], H.L. Russell[238], G. Russo[113,114], J.P. Rutherfoord[8], S. Rutherford Colmenares[46], M. Rybar[193], P. Rybczynski[134], E.B. Rye[179], A. Ryzhov[71], J.A. Sabater Iglesias[83], H.F-W. Sadrozinski[196], F. Safai Tehrani[113], S. Saha[1], M. Sahinsoy[124], B. Sahoo[242], A. Saibel[236], B.T. Saifuddin[174], M. Saimpert[195], M. Saito[225], T. Saito[225], A. Sala[105,106], D. Salamani[61], A. Salnikov[213], J. Salt[236], A. Salvador Salas[223], D. Salvatore[70,69], F. Salvatore[216], A. Salzburger[61], D. Sammel[81], E. Sampson[141], D. Sampsonidis[224,251], D. Sampsonidou[177], J. Sánchez[236], V. Sanchez Sebastian[236], H. Sandaker[179], C.O. Sander[75], J.A. Sandesara[153], M. Sandhoff[244], C. Sandoval[28], L. Sanfilippo[91], D.P.C. Sankey[194], T. Sano[137], A. Sansoni[80], L. Santi[61], C. Santoni[66], H. Santos[184,185], A. Santra[242], E. Sanzani[29,30], K.A. Saoucha[132], J.G. Saraiva[184,187], J. Sardain[8], O. Sasaki[130], K. Sato[230], C. Sauer[61], E. Sauvan[5], P. Savard[227,281], R. Sawada[225], C. Sawyer[194], L. Sawyer[147], C. Sbarra[30], A. Sbrizzi[29,30], T. Scanlon[146], J. Schaarschmidt[204], U. Schäfer[150], A.C. Schaffer[71,97], D. Schaile[159], R.D. Schamberger[215], C. Scharf[21], M.M. Schefer[22], V.A. Schegelsky[63], D. Scheirich[193], M. Schernau[201], C. Scheulen[83], C. Schiavi[85,84], M. Schioppa[70,69], B. Schlag[213], S. Schlenker[61], J. Schmeing[244], M.A. Schmidt[244], K. Schmieden[150], C. Schmitt[150], N. Schmitt[150], S. Schmitt[75], L. Schoeffel[195], A. Schoening[92], P.G. Scholer[54], E. Schopf[211], M. Schott[31], S. Schramm[83], T. Schroer[83], H-C. Schultz-Coulon[91], M. Schumacher[81], B.A. Schumm[196], Ph. Schune[195], H.R. Schwartz[196], A. Schwartzman[213], T.A. Schwarz[156], Ph. Schwemling[195], R. Schwienhorst[157], F.G. Sciacca[22], A. Sciandra[43], G. Sciolla[33], F. Scuri[111], C.D. Sebastiani[61], K. Sedlaczek[168], S.C. Seidel[165], A. Seiden[196], B.D. Seidlitz[67], C. Seitz[75], J.M. Seixas[126], G. Sekhniaidze[107], L. Selem[88], N. Semprini-Cesari[29,30], A. Semushin[63,246], D. Sengupta[83], V. Senthilkumar[236], L. Serin[97], M. Sessa[115,116], H. Severini[174], F. Sforza[85,84], A. Sfyrla[83], Q. Sha[15], E. Shabalina[82], H. Shaddix[168], A.H. Shah[46], R. Shaheen[214], J.D. Shahinian[182], D. Shaked Renous[242], M. Shamim[61], L.Y. Shan[15], M. Shapiro[19], A. Sharma[61], A.S. Sharma[237], P. Sharma[43], P.B. Shatalov[63], K. Shaw[216], S.M. Shaw[151], Q. Shen[207], D.J. Sheppard[212], P. Sherwood[146], L. Shi[146], X. Shi[15], S. Shimizu[130], C.O. Shimmin[245], I.P.J. Shipsey[180,289], S. Shirabe[138], M. Shiyakova[64,272], M.J. Shochet[65], D.R. Shope[179], B. Shrestha[174], S. Shrestha[173,287], I. Shreyber[64], M.J. Shroff[238], P. Sicho[191], A.M. Sickles[235], E. Sideras Haddad[53,233], A.C. Sidley[167], A. Sidoti[30], F. Siegert[77], Dj. Sijacki[17], F. Sili[140], J.M. Silva[79], I. Silva Ferreira[126], M.V. Silva Oliveira[43], S.B. Silverstein[73], S. Simion[97], R. Simoniello[61], E.L. Simpson[151], H. Simpson[216], L.R. Simpson[156], S. Simsek[124], S. Sindhu[82], P. Sinervo[227], S.N. Singh[33], S. Singh[43], S. Sinha[75], S. Sinha[151], M. Sioli[30,29], K. Sioulas[10], I. Siral[61], E. Sitnikova[75], J. Sjölin[73,74], A. Skaf[82], E. Skorda[23], P. Skubic[174], M. Slawinska[136], I. Slazyk[18], V. Smakhtin[242], B.H. Smart[194], S.Yu. Smirnov[198], Y. Smirnov[124], L.N. Smirnova[63,247], O. Smirnova[148], A.C. Smith[67], D.R. Smith[232], E.A. Smith[65], J.L. Smith[151], M.B. Smith[54], R. Smith[213], H. Smitmanns[150], M. Smizanska[141], K. Smolek[192], P. Smolyanskiy[192], A.A. Snesarev[64], H.L. Snoek[167], S. Snyder[43], R. Sobie[238,274], A. Soffer[223], C.A. Solans Sanchez[61], E.Yu. Soldatov[64], U. Soldevila[236], A.A. Solodkov[53], S. Solomon[33], A. Soloshenko[64], K. Solovieva[81], O.V. Solovyanov[66], P. Sommer[77], A. Sonay[14], W.Y. Song[229], A. Sopczak[192], A.L. Sopio[79], F. Sopkova[42], J.D. Sorenson[165], I.R. Sotarriva Alvarez[203], V. Sothilingam[91], O.J. Soto Sandoval[198,199], S. Sottocornola[99], R. Soualah[131], Z. Soumaimi[59], D. South[75], N. Soybelman[242], S. Spagnolo[103,104], M. Spalla[160], D. Sperlich[81], B. Spisso[107,108], D.P. Spiteri[87], L. Splendori[152], M. Spousta[193], E.J. Staats[54], R. Stamen[91], E. Stanecka[136], W. Stanek-Maslouska[75], M.V. Stange[77], B. Stanislaus[19], M.M. Stanitzki[75], B. Stapf[75], E.A. Starchenko[63], G.H. Stark[196], J. Stark[139], P. Staroba[191], P. Starovoitov[132], R. Staszewski[136], G. Stavropoulos[72], A. Stefl[61], P. Steinberg[43], B.

Stelzer[212,228], H.J. Stelzer[183], O. Stelzer[228], H. Stenzel[86], T.J. Stevenson[216], G.A. Stewart[61], J.R. Stewart[175], M.C. Stockton[61], G. Stoicea[35], M. Stolarski[184], S. Stonjek[160], A. Straessner[77], J. Strandberg[214], S. Strandberg[73,74], M. Stratmann[244], M. Strauss[174], T. Strebler[152], P. Strizenec[42], R. Ströhmer[239], D.M. Strom[177], R. Stroynowski[71], A. Strubig[73,74], S.A. Stucci[43], B. Stugu[18], J. Stupak[174], N.A. Styles[75], D. Su[213], S. Su[90], W. Su[208], X. Su[90], D. Suchy[41], K. Sugizaki[182], V.V. Sulin[63], M.J. Sullivan[142], D.M.S. Sultan[180], L. Sultanaliyeva[63], S. Sultansoy[4], S. Sun[243], W. Sun[15], O. Sunneborn Gudnadottir[234], N. Sur[152], M.R. Sutton[216], H. Suzuki[230], M. Svatos[191], P.N. Swallow[46], M. Swiatlowski[228], T. Swirski[239], I. Sykora[41], M. Sykora[193], T. Sykora[193], D. Ta[150], K. Tackmann[75,271], A. Taffard[232], R. Tafirout[228], Y. Takubo[130], M. Talby[152], A.A. Talyshev[63], K.C. Tam[94], N.M. Tamir[223], A. Tanaka[225], J. Tanaka[225], R. Tanaka[97], M. Tanasini[215], Z. Tao[237], S. Tapia Araya[202], S. Tapprogge[150], A. Tarek Abouelfadl Mohamed[157], S. Tarem[222], K. Tariq[15], G. Tarna[35], G.F. Tartarelli[105], M.J. Tartarin[139], P. Tas[193], M. Tasevsky[191], E. Tassi[69,70], A.C. Tate[235], G. Tateno[225], Y. Tayalati[59,273], G.N. Taylor[155], W. Taylor[229], A.S. Tegetmeier[139], P. Teixeira-Dias[145], J.J. Teoh[227], K. Terashi[225], J. Terron[149], S. Terzo[14], M. Testa[80], R.J. Teuscher[227,274], A. Thaler[121], O. Theiner[83], T. Theveneaux-Pelzer[152], O. Thielmann[244], D.W. Thomas[145], J.P. Thomas[23], E.A. Thompson[19], P.D. Thompson[23], E. Thomson[182], R.E. Thornberry[71], C. Tian[90], Y. Tian[83], V. Tikhomirov[124], Yu.A. Tikhonov[63], S. Timoshenko[63], D. Timoshyn[193], E.X.L. Ting[1], P. Tipton[245], A. Tishelman-Charny[43], S.H. Tlou[53], K. Todome[203], S. Todorova-Nova[193], S. Todt[77], L. Toffolin[100,102], M. Togawa[130], J. Tojo[138], S. Tokár[41], O. Toldaiev[99], G. Tolkachev[152], M. Tomoto[130,161], L. Tompkins[213,261], E. Torrence[177], H. Torres[139], E. Torró Pastor[236], M. Toscani[44], C. Tosciri[65], M. Tost[12], D.R. Tovey[209], T. Trefzger[239], P.M. Tricarico[14], A. Tricoli[43], I.M. Trigger[228], S. Trincaz-Duvoid[181], D.A. Trischuk[33], A. Tropina[64], L. Truong[49], M. Trzebinski[136], A. Trzupek[136], F. Tsai[215], M. Tsai[156], A. Tsiamis[224], P.V. Tsiareshka[64], S. Tsigaridas[228], A. Tsirigotis[224,267], V. Tsiskaridze[227], E.G. Tskhadadze[219], M. Tsopoulou[224], Y. Tsujikawa[137], I.I. Tsukerman[63], V. Tsulaia[19], S. Tsuno[130], K. Tsuri[172], D. Tsybychev[215], Y. Tu[94], A. Tudorache[35], V. Tudorache[35], S. Turchikhin[84,85], I. Turk Cakir[3], R. Turra[105], T. Turtuvshin[64,275], P.M. Tuts[67], S. Tzamarias[224,251], E. Tzovara[150], Y. Uematsu[130], F. Ukegawa[230], P.A. Ulloa Poblete[198,199], E.N. Umaka[43], G. Unal[61], A. Undrus[43], G. Unel[232], J. Urban[42], P. Urrejola[197], G. Usai[9], R. Ushioda[226], M. Usman[158], F. Ustuner[79], Z. Uysal[124], V. Vacek[192], B. Vachon[154], T. Vafeiadis[61], A. Vaitkus[146], C. Valderanis[159], E. Valdes Santurio[73,74], M. Valente[228], S. Valentinetti[29,30], A. Valero[236], E. Valiente Moreno[236], A. Vallier[139], J.A. Valls Ferrer[236], D.R. Van Arneman[167], T.R. Van Daalen[204], A. Van Der Graaf[76], H.Z. Van Der Schyf[53], P. Van Gemmeren[7], M. Van Rijnbach[61], S. Van Stroud[146], I. Van Vulpen[167], P. Vana[193], M. Vanadia[115,116], U.M. Vande Voorde[214], W. Vandelli[61], E.R. Vandewall[175], D. Vannicola[223], L. Vannoli[80], R. Vari[113], E.W. Varnes[8], C. Varni[20], D. Varouchas[97], L. Varriale[236], K.E. Varvell[217], M.E. Vasile[35], L. Vaslin[130], M.D. Vassilev[213], A. Vasyukov[64], L.M. Vaughan[175], R. Vavricka[193], T. Vazquez Schroeder[14], J. Veatch[45], V. Vecchio[151], M.J. Veen[153], I. Veliscek[43], L.M. Veloce[227], F. Veloso[184,186], S. Veneziano[113], A. Ventura[103,104], S. Ventura Gonzalez[195], A. Verbytskyi[160], M. Verducci[111,112], C. Vergis[144], M. Verissimo De Araujo[126], W. Verkerke[167], J.C. Vermeulen[167], C. Vernieri[213], M. Vessella[232], M.C. Vetterli[212,281], A. Vgenopoulos[150], N. Viaux Maira[202], T. Vickey[209], O.E. Vickey Boeriu[209], G.H.A. Viehhauser[180], L. Vigani[92], M. Vigl[160], M. Villa[30,29], M. Villaplana Perez[236], E.M. Villhauer[79], E. Vilucchi[80], M.G. Vincter[54], A. Visibile[167], C. Vittori[61], I. Vivarelli[29,30], E. Voevodina[160], F. Vogel[159], J.C. Voigt[77], P. Vokac[192], Yu. Volkotrub[135], E. Von Toerne[31], B. Vormwald[61], K. Vorobev[78], M. Vos[236], K. Voss[211], M. Vozak[61], L. Vozdecky[174], N. Vranjes[17], M. Vranjes Milosavljevic[17], M. Vreeswijk[167], N.K. Vu[207,208], R. Vuillermet[61], O. Vujinovic[150], I. Vukotic[65], I.K. Vyas[54], J.F. Wack[46], S. Wada[230], C. Wagner[213], J.M. Wagner[19], W. Wagner[244], S. Wahdan[244], H. Wahlberg[140], C.H. Waits[174], J. Walder[194], R. Walker[159], W. Walkowiak[211], A. Wall[182], E.J. Wallin[148], T. Wamorkar[19], A.Z. Wang[196], C. Wang[150], C. Wang[12], H. Wang[19], J. Wang[95], P. Wang[151], P. Wang[146], R. Wang[89], R. Wang[7], S.M. Wang[218], S. Wang[15], T. Wang[90], T. Wang[90], W.T. Wang[122], W. Wang[15], X. Wang[235], X. Wang[207], X. Wang[75], Y. Wang[162], Y. Wang[90], Z. Wang[156], Z. Wang[78,207,208], Z. Wang[156], C. Wanotayaroj[130], A. Warburton[154], A.L. Warnerbring[211], N. Warrack[87], S. Waterhouse[145], A.T. Watson[23], H. Watson[79], M.F. Watson[23], E. Watton[87], G. Watts[204], B.M. Waugh[146], J.M. Webb[81], C. Weber[43], H.A. Weber[21], M.S. Weber[22], S.M. Weber[91], C. Wei[90], Y. Wei[81], A.R. Weidberg[180], E.J. Weik[171], J. Weingarten[76], C. Weiser[81], C.J. Wells[75], T. Wenaus[43], B. Wendland[76], T. Wengler[61], N.S. Wenke[160], N. Wermes[31], M. Wessels[91], A.M. Wharton[141], A.S. White[89], A. White[9], M.J. White[1], D. Whiteson[232], L. Wickremasinghe[178], W. Wiedenmann[243], M. Wielers[194], C. Wiglesworth[68], D.J. Wilbern[174], H.G. Wilkens[61], J.J.H. Wilkinson[46], D.M. Williams[67], H.H. Williams[182], S. Williams[46], S. Willocq[153], B.J. Wilson[151], D.J. Wilson[151], P.J. Windischhofer[65], F.I. Winkel[44], F. Winklmeier[177], B.T. Winter[81], M. Wittgen[213], M. Wobisch[147], T. Wojtkowski[88], Z. Wolffs[167], J. Wollrath[61], M.W. Wolter[136], H. Wolters[184,186], M.C. Wong[196], E.L. Woodward[67], S.D. Worm[75], B.K. Wosiek[136], K.W. Woźniak[136], S. Wozniewski[82], K. Wraight[87], C. Wu[23], M. Wu[163], M. Wu[166], S.L. Wu[243], S. Wu[15], X. Wu[83], X. Wu[90], Y. Wu[90], Z. Wu[5], J. Wuerzinger[160,279], T.R. Wyatt[151], B.M. Wynne[79], S. Xella[68], L. Xia[162], M. Xia[16], M. Xie[90], A. Xiong[177], J. Xiong[19], D. Xu[15], H. Xu[90], L. Xu[90], R. Xu[182], T. Xu[156], Y. Xu[204], Z. Xu[79], Z. Xu[162], B. Yabsley[217], S. Yacoob[47], Y. Yamaguchi[130], E. Yamashita[225], H. Yamauchi[230], T. Yamazaki[19], Y. Yamazaki[133], S. Yan[87], Z. Yan[153], H.J. Yang[207,208], H.T. Yang[90], S. Yang[90], T. Yang[95], X. Yang[61], X. Yang[15], Y. Yang[225], Y. Yang[90], W-M. Yao[19], C.L. Yardley[216], H. Ye[82], J. Ye[15], S. Ye[43], X. Ye[90], Y. Yeh[146], I. Yeletskikh[64], B. Yeo[20], M.R. Yexley[146], T.P. Yildirim[180], P. Yin[67], K. Yorita[241], S. Younas[35], C.J.S. Young[61], C. Young[213], N.D. Young[177], Y. Yu[90], J. Yuan[15,164,283], M. Yuan[156], R. Yuan[208,207], L. Yue[146], M. Zaazoua[90], B. Zabinski[136], I. Zahir[55], A. Zaio[84,85], Z.K. Zak[136], T. Zakareishvili[236], S. Zambito[83], J.A. Zamora Saa[200], J. Zang[225], D. Zanzi[81], R. Zanzottera[105,106], O. Zaplatilek[192], C. Zeitnitz[244], H. Zeng[15], J.C. Zeng[235], D.T. Zenger Jr[33], O. Zenin[63], T. Ženiš[41], S. Zenz[144], S. Zerradi[55], D. Zerwas[97], M. Zhai[15,164], D.F. Zhang[209], J. Zhang[205], J. Zhang[7], K. Zhang[15,164], L. Zhang[90], L. Zhang[162], P. Zhang[15,164], R. Zhang[243], S. Zhang[139], T. Zhang[225], X. Zhang[207], Y. Zhang[204], Y. Zhang[146], Y. Zhang[90], Y. Zhang[162], Z. Zhang[19], Z. Zhang[205], Z. Zhang[97], H. Zhao[204], T. Zhao[205], Y. Zhao[54], Z. Zhao[90], Z. Zhao[90], A. Zhemchugov[64], J. Zheng[162], K. Zheng[235], X. Zheng[90], Z. Zheng[213], D. Zhong[235], B. Zhou[156], H. Zhou[8], N. Zhou[207], Y. Zhou[16], Y. Zhou[162], Y. Zhou[8], C.G. Zhu[205], J. Zhu[156], X. Zhu[208], Y. Zhu[207], Y. Zhu[90], X. Zhuang[15], K. Zhukov[99], N.I. Zimine[64], J. Zinsser[92], M. Ziolkowski[211], L. Živković[17], A. Zoccoli[29,30], K. Zoch[89], T.G. Zorbas[209], W. Zou[67], L. Zwalinski[61]

Collaboration Institutes

[1] Department of Physics, University of Adelaide, Adelaide, Australia
[2] Department of Physics, University of Alberta, Edmonton, AB, Canada
[3] Department of Physics, Ankara University, Ankara, Türkiye
[4] Division of Physics, TOBB University of Economics and Technology, Ankara, Türkiye

[5] LAPP, Université Savoie Mont Blanc, CNRS/IN2P3, Annecy, France
[6] APC, Université Paris Cité, CNRS/IN2P3, Paris, France
[7] High Energy Physics Division, Argonne National Laboratory, Argonne, IL, United States of America
[8] Department of Physics, University of Arizona, Tucson, AZ, United States of America
[9] Department of Physics, University of Texas at Arlington, Arlington, TX, United States of America
[10] Physics Department, National and Kapodistrian University of Athens, Athens, Greece
[11] Physics Department, National Technical University of Athens, Zografou, Greece
[12] Department of Physics, University of Texas at Austin, Austin, TX, United States of America
[13] Institute of Physics, Azerbaijan Academy of Sciences, Baku, Azerbaijan
[14] Institut de Física d'Altes Energies (IFAE), Barcelona Institute of Science and Technology, Barcelona, Spain
[15] Institute of High Energy Physics, Chinese Academy of Sciences, Beijing, China
[16] Physics Department, Tsinghua University, Beijing, China
[17] Institute of Physics, University of Belgrade, Belgrade, Serbia
[18] Department for Physics and Technology, University of Bergen, Bergen, Norway
[19] Physics Division, Lawrence Berkeley National Laboratory, Berkeley, CA, United States of America
[20] University of California, Berkeley, CA, United States of America
[21] Institut für Physik, Humboldt Universität zu Berlin, Berlin, Germany
[22] Albert Einstein Center for Fundamental Physics and Laboratory for High Energy Physics, University of Bern, Bern, Switzerland
[23] School of Physics and Astronomy, University of Birmingham, Birmingham, United Kingdom
[24] Department of Physics, Bogazici University, Istanbul, Türkiye
[25] Department of Physics Engineering, Gaziantep University, Gaziantep, Türkiye
[26] Department of Physics, Istanbul University, Istanbul, Türkiye
[27] Facultad de Ciencias y Centro de Investigaciónes, Universidad Antonio Nariño, Bogotá, Colombia
[28] Departamento de Física, Universidad Nacional de Colombia, Bogotá, Colombia
[29] Dipartimento di Fisica e Astronomia A. Righi, Università di Bologna, Bologna, Italy
[30] INFN Sezione di Bologna, Italy
[31] Physikalisches Institut, Universität Bonn, Bonn, Germany
[32] Department of Physics, Boston University, Boston, MA, United States of America
[33] Department of Physics, Brandeis University, Waltham, MA, United States of America
[34] Transilvania University of Brasov, Brasov, Romania
[35] Horia Hulubei National Institute of Physics and Nuclear Engineering, Bucharest, Romania
[36] Department of Physics, Alexandru Ioan Cuza University of Iasi, Iasi, Romania
[37] Development of Isotopic and Molecular Technologies, Physics Department, National Institute for Research, Cluj-Napoca, Romania
[38] National University of Science and Technology Politechnica, Bucharest, Romania
[39] West University in Timisoara, Timisoara, Romania
[40] Faculty of Physics, University of Bucharest, Bucharest, Romania
[41] Faculty of Mathematics, Physics and Informatics, Comenius University, Bratislava, Slovak Republic
[42] Department of Subnuclear Physics, Institute of Experimental Physics, Slovak Academy of Sciences, Kosice, Slovak Republic
[43] Physics Department, Brookhaven National Laboratory, Upton, NY, United States of America
[44] Facultad de Ciencias Exactas y Naturales, Departamento de Física, Instituto de Física de Buenos Aires (IFIBA), CONICET, Universidad de Buenos Aires, Buenos Aires, Argentina
[45] California State University, CA, United States of America
[46] Cavendish Laboratory, University of Cambridge, Cambridge, United Kingdom
[47] Department of Physics, University of Cape Town, Cape Town, South Africa
[48] iThemba Labs, Western Cape, South Africa
[49] Department of Mechanical Engineering Science, University of Johannesburg, Johannesburg, South Africa
[50] National Institute of Physics, University of The Philippines Diliman, Philippines, South Africa
[51] Department of Physics, University of South Africa, Pretoria, South Africa
[52] University of Zululand, KwaDlangezwa, South Africa
[53] School of Physics, University of the Witwatersrand, Johannesburg, South Africa
[54] Department of Physics, Carleton University, Ottawa, ON, Canada
[55] Faculté des Sciences Ain Chock, Université Hassan II de Casablanca, Morocco
[56] Faculté des Sciences, Kénitra, Université Ibn-Tofail, Morocco
[57] Faculté des Sciences Semlalia, Université Cadi Ayyad, LPHEA-Marrakech, Morocco
[58] Faculté des Sciences, LPMR, Université Mohamed Premier, Oujda, Morocco
[59] Faculté des sciences, Université Mohammed V, Rabat, Morocco
[60] Institute of Applied Physics, Mohammed VI Polytechnic University, Ben Guerir, Morocco
[61] CERN, Geneva, Switzerland
[62] Affiliated with an institute formerly covered by a cooperation agreement with CERN
[63] Affiliated with an institute covered by a cooperation agreement with CERN
[64] Affiliated with an international laboratory covered by a cooperation agreement with CERN
[65] Enrico Fermi Institute, University of Chicago, Chicago, IL, United States of America
[66] LPC, Université Clermont Auvergne, CNRS/IN2P3, Clermont-Ferrand, France
[67] Nevis Laboratory, Columbia University, Irvington, NY, United States of America
[68] Niels Bohr Institute, University of Copenhagen, Copenhagen, Denmark
[69] Dipartimento di Fisica, Università della Calabria, Rende, Italy
[70] INFN Gruppo Collegato di Cosenza, Laboratori Nazionali di Frascati, Italy
[71] Physics Department, Southern Methodist University, Dallas, TX, United States of America
[72] National Centre for Scientific Research Demokritos, Agia Paraskevi, Greece
[73] Department of Physics, Stockholm University, Sweden
[74] Oskar Klein Centre, Stockholm, Sweden
[75] Deutsches Elektronen-Synchrotron DESY, Hamburg and Zeuthen, Germany
[76] Fakultät Physik, Technische Universität Dortmund, Dortmund, Germany
[77] Institut für Kern- und Teilchenphysik, Technische Universität Dresden, Dresden, Germany
[78] Department of Physics, Duke University, Durham, NC, United States of America
[79] SUPA - School of Physics and Astronomy, University of Edinburgh, Edinburgh, United Kingdom
[80] INFN e Laboratori Nazionali di Frascati, Frascati, Italy
[81] Physikalisches Institut, Albert-Ludwigs-Universität Freiburg, Freiburg, Germany

[82] II. Physikalisches Institut, Georg-August-Universität Göttingen, Göttingen, Germany
[83] Département de Physique Nucléaire et Corpusculaire, Université de Genève, Genève, Switzerland
[84] Dipartimento di Fisica, Università di Genova, Genova, Italy
[85] INFN Sezione di Genova, Italy
[86] II. Physikalisches Institut, Justus-Liebig-Universität Giessen, Giessen, Germany
[87] SUPA - School of Physics and Astronomy, University of Glasgow, Glasgow, United Kingdom
[88] LPSC, Université Grenoble Alpes, CNRS/IN2P3, Grenoble INP, Grenoble, France
[89] Laboratory for Particle Physics and Cosmology, Harvard University, Cambridge, MA, United States of America
[90] Department of Modern Physics and State Key Laboratory of Particle Detection and Electronics, University of Science and Technology of China, Hefei, China
[91] Kirchhoff-Institut für Physik, Ruprecht-Karls-Universität Heidelberg, Heidelberg, Germany
[92] Physikalisches Institut, Ruprecht-Karls-Universität Heidelberg, Heidelberg, Germany
[93] Department of Physics, Chinese University of Hong Kong, Shatin Hong Kong, N.T, China
[94] Department of Physics, University of Hong Kong, Hong Kong, China
[95] Department of Physics, Institute for Advanced Study, Hong Kong University of Science and Technology, Clear Water Bay, Kowloon, Hong Kong, China
[96] Department of Physics, National Tsing Hua University, Hsinchu, Taiwan
[97] IJCLab, Université Paris-Saclay, CNRS/IN2P3, 91405, Orsay, France
[98] Centro Nacional de Microelectrónica (IMB-CNM-CSIC), Barcelona, Spain
[99] Department of Physics, Indiana University, Bloomington, IN, United States of America
[100] INFN Gruppo Collegato di Udine, Sezione di Trieste, Udine, Italy
[101] ICTP, Trieste, Italy
[102] Dipartimento Politecnico di Ingegneria e Architettura, Università di Udine, Udine, Italy
[103] INFN Sezione di Lecce, Italy
[104] Dipartimento di Matematica e Fisica, Università del Salento, Lecce, Italy
[105] INFN Sezione di Milano, Italy
[106] Dipartimento di Fisica, Università di Milano, Milano, Italy
[107] INFN Sezione di Napoli, Italy
[108] Dipartimento di Fisica, Università di Napoli, Napoli, Italy
[109] INFN Sezione di Pavia, Italy
[110] Dipartimento di Fisica, Università di Pavia, Pavia, Italy
[111] INFN Sezione di Pisa, Italy
[112] Dipartimento di Fisica E. Fermi, Università di Pisa, Pisa, Italy
[113] INFN Sezione di Roma, Italy
[114] Dipartimento di Fisica, Sapienza Università di Roma, Roma, Italy
[115] INFN Sezione di Roma Tor Vergata, Italy
[116] Dipartimento di Fisica, Università di Roma Tor Vergata, Roma, Italy
[117] INFN Sezione di Roma Tre, Italy
[118] Dipartimento di Matematica e Fisica, Università Roma Tre, Roma, Italy
[119] INFN-TIFPA, Italy
[120] Università degli Studi di Trento, Trento, Italy
[121] Department of Astro and Particle Physics, Universität Innsbruck, Innsbruck, Austria
[122] University of Iowa, Iowa City, IA, United States of America
[123] Department of Physics and Astronomy, Iowa State University, Ames, IA, United States of America
[124] Istinye University, Sariyer Istanbul, Türkiye
[125] Departamento de Engenharia Elétrica, Universidade Federal de Juiz de Fora (UFJF), Juiz de Fora, Brazil
[126] COPPE/EE/IF, Universidade Federal do Rio, De Janeiro Rio de Janeiro, Brazil
[127] Instituto de Física, Universidade de São Paulo, São Paulo, Brazil
[128] Janeiro State University, Rio de Janeiro, Brazil
[129] Federal University of Bahia, Bahia, Brazil
[130] KEK, High Energy Accelerator Research Organization, Tsukuba, Japan
[131] Khalifa University of Science and Technology, Abu Dhabi, United Arab Emirates
[132] University of Sharjah, Sharjah, United Arab Emirates
[133] Graduate School of Science, Kobe University, Kobe, Japan
[134] Faculty of Physics and Applied Computer Science, AGH University of Krakow, Krakow, Poland
[135] Marian Smoluchowski Institute of Physics, Jagiellonian University, Krakow, Poland
[136] Institute of Nuclear Physics, Polish Academy of Sciences, Krakow, Poland
[137] Faculty of Science, Kyoto University, Kyoto, Japan
[138] Research Center for Advanced Particle Physics, Department of Physics, Kyushu University, Fukuoka, Japan
[139] L2IT, Université de Toulouse, CNRS/IN2P3, UPS, Toulouse, France
[140] Instituto de Física La Plata, Universidad Nacional de La Plata and CONICET, La Plata, Argentina
[141] Physics Department, Lancaster University, Lancaster, United Kingdom
[142] Oliver Lodge Laboratory, University of Liverpool, Liverpool, United Kingdom
[143] Department of Experimental Particle Physics, Department of Physics, Jožef Stefan Institute, University of Ljubljana, Ljubljana, Slovenia
[144] Department of Physics and Astronomy, Queen Mary University of London, London, United Kingdom
[145] Department of Physics, Royal Holloway University of London, Egham, United Kingdom
[146] Department of Physics and Astronomy, University College London, London, United Kingdom
[147] Louisiana Tech University, Ruston, LA, United States of America
[148] Fysiska institutionen, Lunds universitet, Lund, Sweden
[149] Departamento de Física Teorica C-15 and CIAFF, Universidad Autónoma de Madrid, Madrid, Spain
[150] Institut für Physik, Universität Mainz, Mainz, Germany
[151] School of Physics and Astronomy, University of Manchester, Manchester, United Kingdom
[152] CPPM, Aix-Marseille Université, CNRS/IN2P3, Marseille, France
[153] Department of Physics, University of Massachusetts, Amherst, MA, United States of America
[154] Department of Physics, McGill University, Montreal, QC, Canada
[155] School of Physics, University of Melbourne, Victoria, Australia
[156] Department of Physics, University of Michigan, Ann Arbor, MI, United States of America
[157] Department of Physics and Astronomy, Michigan State University, East Lansing, MI, United States of America
[158] Group of Particle Physics, University of Montreal, Montreal, QC, Canada
[159] Fakultät für Physik, Ludwig-Maximilians-Universität München, München, Germany
[160] Max-Planck-Institut für Physik (Werner-Heisenberg-Institut), München, Germany
[161] Graduate School of Science and Kobayashi-Maskawa Institute, Nagoya University, Nagoya, Japan
[162] Department of Physics, Nanjing University, Nanjing, China
[163] School of Science, Shenzhen Campus of Sun Yat-sen University, China
[164] University of Chinese Academy of Science (UCAS), Beijing, China
[165] Department of Physics and Astronomy, University of New Mexico, Albuquerque, NM, United States of America

[166] Institute for Mathematics, Astrophysics and Particle Physics, Radboud University/Nikhef, Nijmegen, Netherlands
[167] Nikhef National Institute for Subatomic Physics and University of Amsterdam, Amsterdam, Netherlands
[168] Department of Physics, Northern Illinois University, DeKalb, IL, United States of America
[169] New York University Abu Dhabi, Abu Dhabi, United Arab Emirates
[170] United Arab Emirates University, Al Ain, United Arab Emirates
[171] Department of Physics, New York University, New York, NY, United States of America
[172] Ochanomizu University, Otsuka, Bunkyo-ku, Tokyo, Japan
[173] Ohio State University, Columbus, OH, United States of America
[174] Department of Physics and Astronomy, Homer L. Dodge, University of Oklahoma, Norman, OK, United States of America
[175] Department of Physics, Oklahoma State University, Stillwater, OK, United States of America
[176] Joint Laboratory of Optics, Palacký University, Olomouc, Czech Republic
[177] Institute for Fundamental Science, University of Oregon, Eugene, OR, United States of America
[178] Graduate School of Science, University of Osaka, Osaka, Japan
[179] Department of Physics, University of Oslo, Oslo, Norway
[180] Department of Physics, Oxford University, Oxford, United Kingdom
[181] LPNHE, Sorbonne Université, Université Paris Cité, CNRS/IN2P3, Paris, France
[182] Department of Physics, University of Pennsylvania, Philadelphia, PA, United States of America
[183] Department of Physics and Astronomy, University of Pittsburgh, Pittsburgh, PA, United States of America
[184] Laboratório de Instrumentação e Física Experimental de Partículas - LIP, Lisboa, Portugal
[185] Departamento de Física, Faculdade de Ciências, Universidade de Lisboa, Lisboa, Portugal
[186] Departamento de Física, Universidade de Coimbra, Coimbra, Portugal
[187] Centro de Física Nuclear da Universidade de Lisboa, Lisboa, Portugal
[188] Departamento de Física, Escola de Ciências, Universidade do Minho, Braga, Portugal
[189] Departamento de Física Teórica y del Cosmos, Universidad de Granada, Granada, Spain
[190] Departamento de Física, Instituto Superior Técnico, Universidade de Lisboa, Lisboa, Portugal
[191] Institute of Physics, Czech Academy of Sciences, Prague, Czech Republic
[192] Czech Technical University, Prague Prague, Czech Republic
[193] Faculty of Mathematics and Physics, Charles University, Prague, Czech Republic
[194] Particle Physics Department, Rutherford Appleton Laboratory Didcot, United Kingdom
[195] IRFU, CEA, Université Paris-Saclay, Gif-sur-Yvette, France
[196] Santa Cruz Institute for Particle Physics, University of California Santa Cruz, Santa Cruz, CA, United States of America
[197] Departamento de Física, Pontificia Universidad Católica de Chile, Santiago, Chile
[198] Millennium Institute for Subatomic physics at high energy frontier (SAPHIR), Santiago, Chile
[199] Departamento de Física, Instituto de Investigación Multidisciplinario en Ciencia y Tecnología, Universidad de La Serena, Chile
[200] Department of Physics, Universidad Andres Bello, Santiago, Chile
[201] Instituto de Alta Investigación, Universidad de Tarapacá, Arica, Chile
[202] Departamento de Física, Universidad Técnica Federico Santa María, Valparaíso, Chile
[203] Department of Physics, Institute of Science, Tokyo, Japan
[204] Department of Physics, University of Washington, Seattle, WA, United States of America
[205] Institute of Frontier and Interdisciplinary Science and Key, Laboratory of Particle Physics and Particle Irradiation (MOE), Shandong University, Qingdao, China
[206] School of Physics, Zhengzhou University, China
[207] School of Physics and Astronomy, State Key Laboratory of Dark Matter Physics, Shanghai Jiao Tong University, Key Laboratory for Particle Astrophysics and Cosmology (MOE), SKLPPC, Shanghai, China
[208] State Key Laboratory of Dark Matter Physics, Tsung-Dao Lee Institute, Shanghai Jiao Tong University, Shanghai, China
[209] Department of Physics and Astronomy, University of Sheffield, Sheffield, United Kingdom
[210] Department of Physics, Shinshu University, Nagano, Japan
[211] Department Physik, Universität Siegen, Siegen, Germany
[212] Department of Physics, Simon Fraser University, Burnaby, BC, Canada
[213] SLAC National Accelerator Laboratory, Stanford, CA, United States of America
[214] Department of Physics, Royal Institute of Technology, Stockholm, Sweden
[215] Departments of Physics and Astronomy, Stony Brook University, Stony Brook, NY, United States of America
[216] Department of Physics and Astronomy, University of Sussex, Brighton, United Kingdom
[217] School of Physics, University of Sydney, Sydney, Australia
[218] Institute of Physics, Academia Sinica, Taipei, Taiwan
[219] E. Andronikashvili Institute of Physics, Iv. Javakhishvili Tbilisi State University, Tbilisi, Georgia
[220] High Energy Physics Institute, Tbilisi State University, Tbilisi, Georgia
[221] University of Georgia, Tbilisi, Georgia
[222] Department of Physics, Israel Institute of Technology, Technion Haifa, Israel
[223] Raymond and Beverly Sackler School of Physics and Astronomy, Tel Aviv University, Tel Aviv, Israel
[224] Department of Physics, Aristotle University of Thessaloniki, Thessaloniki, Greece
[225] International Center for Elementary Particle Physics, Department of Physics, University of Tokyo, Tokyo, Japan
[226] Graduate School of Science and Technology, Tokyo Metropolitan University, Tokyo, Japan
[227] Department of Physics, University of Toronto, Toronto, ON, Canada
[228] TRIUMF, Vancouver, BC, Canada
[229] Department of Physics and Astronomy, York University, Toronto, ON, Canada
[230] Division of Physics and Tomonaga Center, Faculty of Pure and Applied Sciences, the History of the Universe, University of Tsukuba, Tsukuba, Japan
[231] Department of Physics and Astronomy, Tufts University, Medford, MA, United States of America
[232] Department of Physics and Astronomy, University of California Irvine, Irvine, CA, United States of America
[233] University of West Attica, Athens, Greece
[234] Department of Physics and Astronomy, University of Uppsala, Uppsala, Sweden
[235] Department of Physics, University of Illinois, Urbana, IL, United States of America
[236] Centro Mixto, Instituto de Física Corpuscular (IFIC), Universidad de Valencia - CSIC, Valencia, Spain
[237] Department of Physics, University of British Columbia, Vancouver, BC, Canada
[238] Department of Physics and Astronomy, University of Victoria, Victoria, BC, Canada
[239] Fakultät für Physik und Astronomie, Julius-Maximilians-Universität Würzburg, Würzburg, Germany

[240] Department of Physics, University of Warwick, Coventry, United Kingdom
[241] Waseda University, Tokyo, Japan
[242] Department of Particle Physics and Astrophysics, Weizmann Institute of Science, Rehovot, Israel
[243] Department of Physics, University of Wisconsin, Madison, WI, United States of America
[244] Fachgruppe Physik, Fakultät für Mathematik und Naturwissenschaften, Bergische Universität Wuppertal, Wuppertal, Germany
[245] Department of Physics, Yale University, New Haven, CT, United States of America
[246] Yerevan Physics Institute, Yerevan, Armenia
[247] Also Affiliated with an institute covered by a cooperation agreement with CERN
[248] Also at An-Najah National University, Nablus, Palestine
[249] Also at Borough of Manhattan Community College, University of New York, City, New York NY, United States of America
[250] Also at Center for High Energy Physics, Peking University, China
[251] Also at Center for Interdisciplinary Research and Innovation (CIRI-AUTH), Thessaloniki, Greece
[252] Also at CERN, Geneva, Switzerland
[253] CMD-AC UNEC Research Center, Azerbaijan State University of Economics (UNEC), Azerbaijan
[254] Also at Département de Physique Nucléaire et Corpusculaire, Université de Genève, Genève, Switzerland
[255] Departament de Fisica, Universitat Autonoma de Barcelona, Barcelona, Spain
[256] Department of Financial and Management Engineering, University of the Aegean, Chios, Greece
[257] Department of Mathematical Sciences, University of South Africa, Johannesburg, South Africa
[258] Department of Physics, Bolu Abant Izzet Baysal University, Bolu, Türkiye
[259] Department of Physics, California State University, Sacramento, United States of America
[260] Department of Physics, King's, College London London, United Kingdom
[261] Department of Physics, Stanford University, Stanford, CA, United States of America
[262] Department of Physics, Stellenbosch University, South Africa
[263] Department of Physics, University of Fribourg, Fribourg, Switzerland
[264] Department of Physics, University of Thessaly, Greece
[265] Department of Physics, Westmont College, Santa Barbara, United States of America
[266] Also at Faculty of Physics, Sofia University 'St. Kliment Ohridski', Sofia, Bulgaria
[267] Also at Hellenic Open University, Patras, Greece
[268] Henan University, China
[269] Imam Mohammad Ibn Saud Islamic University, Saudi Arabia
[270] Institucio Catalana de Recerca i Estudis Avancats, ICREA, Barcelona, Spain
[271] Also at Institut für Experimentalphysik, Universität Hamburg, Hamburg, Germany
[272] Also at Institute for Nuclear Research and Nuclear Energy (INRNE), Bulgarian Academy of Sciences, Sofia, Bulgaria
[273] Also at Institute of Applied Physics, Mohammed VI Polytechnic University, Ben Guerir, Morocco
[274] Also at Institute of Particle Physics (IPP), Canada
[275] Also at Institute of Physics and Technology, Mongolian Academy of Sciences, Ulaanbaatar, Mongolia
[276] Also at Institute of Physics, Azerbaijan Academy of Sciences, Baku, Azerbaijan
[277] Also at Institute of Theoretical Physics, Ilia State University, Tbilisi, Georgia
[278] National Institute of Physics, University of the Philippines Diliman (Philippines), Philippines
[279] Technical University of Munich, Munich, Germany
[280] The Collaborative Innovation Center of Quantum Matter (CICQM), Beijing, China
[281] Also at TRIUMF, Vancouver, BC, Canada
[282] Also at Università di Napoli Parthenope, Napoli, Italy
[283] University of Chinese Academy of Sciences (UCAS), Beijing, China
[284] Department of Physics, University of Colorado Boulder, Colorado, United States of America
[285] University of Siena, Italy
[286] Also at University of the Western Cape, South Africa
[287] Also at Washington College, Chestertown, MD, United States of America
[288] Physics Department, Yeditepe University, Istanbul, Türkiye
[289] Deceased

References

[1] ATLAS Collaboration, Observation of a new particle in the search for the standard model Higgs boson with the ATLAS detector at the LHC, Phys. Lett. B 716 (2012) 1. arXiv:1207.7214, https://doi.org/10.1016/j.physletb.2012.08.020
[2] CMS Collaboration, Observation of a new boson at a mass of 125 GeV with the CMS experiment at the LHC, Phys. Lett. B 716 (2012) 30. arXiv:1207.7235, https://doi.org/10.1016/j.physletb.2012.08.021
[3] E. Gabrielli, F. Maltoni, B. Mele, M. Moretti, F. Piccinini, R. Pittau, Higgs boson production in association with a photon in vector boson fusion at the LHC, Nucl. Phys. B 781 (2007) 64–84. arXiv:hep-ph/0702119, https://doi.org/10.1016/j.nuclphysb.2007.05.010
[4] ATLAS Collaboration, Measurements of Higgs bosons decaying to bottom quarks from vector boson fusion production with the ATLAS experiment at $\sqrt{s} = 13$ TeV, Eur. Phys. J. C 81 (2021) 537. arXiv:2011.08280, https://doi.org/10.1140/epjc/s10052-021-09192-8
[5] CMS Collaboration, Measurement of boosted Higgs bosons produced via vector boson fusion or gluon fusion in the $H \to b\bar{b}$ decay mode using LHC proton–proton collision data at $\sqrt{s} = 13$ TeV, JHEP 12 (2024) 035. arXiv:2407.08012, https://doi.org/10.1007/JHEP12(2024)035
[6] ATLAS Collaboration, Search for Higgs boson production in association with a high-energy photon via vector-boson fusion with decay into bottom quark pairs at $\sqrt{s} =$ 13 TeV with the ATLAS detector, JHEP 03 (2021) 268. arXiv:2010.13651, https://doi.org/10.1007/JHEP03(2021)268
[7] B. Denby, Neural networks and cellular automata in experimental high energy physics, Comput. Phys. Commun. 49 (3) (1988) 429–448. https://doi.org/10.1016/0010-4655(88)90004-5
[8] ATLAS Collaboration, The ATLAS experiment at the CERN large hadron collider, JINST 3 (2008) S08003. https://doi.org/10.1088/1748-0221/3/08/S08003
[9] ATLAS Collaboration, Performance of the ATLAS trigger system in 2015, Eur. Phys. J. C 77 (2017) 317. arXiv:1611.09661, https://doi.org/10.1140/epjc/s10052-017-4852-3
[10] ATLAS Collaboration, Software and computing for Run 3 of the ATLAS experiment at the LHC, Eur. Phys. J. C 85 (2025) 234. arXiv:2404.06335, https://doi.org/10.1140/epjc/s10052-024-13701-w
[11] J. Alwall, R. Frederix, S. Frixione, V. Hirschi, F. Maltoni, O. Mattelaer, H.-S. Shao, T. Stelzer, P. Torrielli, M. Zaro, The automated computation of tree-level and next-to-leading order differential cross sections, and their matching to parton shower simulations, JHEP 07 (2014) 079. arXiv:1405.0301, https://doi.org/10.1007/JHEP07(2014)079
[12] M. Bähr, et al., Herwig++ physics and manual, Eur. Phys. J. C 58 (2008) 639. arXiv:0803.0883, https://doi.org/10.1140/epjc/s10052-008-0798-9
[13] J. Bellm, et al., Herwig 7.0/Herwig++ 3.0 release note, Eur. Phys. J. C 76 (4) (2016) 196. arXiv:1512.01178, https://doi.org/10.1140/epjc/s10052-016-4018-8
[14] J. Butterworth, et al., PDF4LHC recommendations for LHC Run II, J. Phys. G 43 (2016) 023001. arXiv:1510.03865, https://doi.org/10.1088/0954-3899/43/2/023001
[15] P. Nason, A new method for combining NLO QCD with shower Monte Carlo algorithms, JHEP 11 (2004) 040. arXiv:hep-ph/0409146, https://doi.org/10.1088/1126-6708/2004/11/040
[16] S. Frixione, P. Nason, C. Oleari, Matching NLO QCD computations with parton shower simulations: the POWHEG method, JHEP 11 (2007) 070. arXiv:0709.2092, https://doi.org/10.1088/1126-6708/2007/11/070
[17] S. Alioli, P. Nason, C. Oleari, E. Re, A general framework for implementing NLO calculations in shower Monte Carlo programs: the POWHEG BOX, JHEP 06 (2010) 043. arXiv:1002.2581, https://doi.org/10.1007/JHEP06(2010)043
[18] T. Sjöstrand, S. Ask, J.R. Christiansen, R. Corke, N. Desai, P. Ilten, S. Mrenna, S. Prestel, C.O. Rasmussen, P.Z. Skands, An introduction to PYTHIA 8.2, Comput. Phys. Commun. 191 (2015) 159. arXiv:1410.3012, https://doi.org/10.1016/j.cpc.2015.01.024
[19] NNPDF Collaboration, R.D. Ball, et al., Parton distributions for the LHC run II, JHEP 04 (2015) 040. arXiv:1410.8849, https://doi.org/10.1007/JHEP04(2015)040

[20] R.D. Ball, et al., The PDF4LHC21 combination of global PDF fits for the LHC Run III, J. Phys. G 49 (2022) 080501. arXiv:2203.05506, https://doi.org/10.1088/1361-6471/ac7216
[21] M. Czakon, A. Mitov, Top++: a program for the calculation of the top-pair cross-section at hadron colliders, Comput. Phys. Commun. 185 (2014) 2930. arXiv:1112.5675, https://doi.org/10.1016/j.cpc.2014.06.021
[22] D.J. Lange, The EvtGen particle decay simulation package, Nucl. Instrum. Meth. A 462 (2001) 152. https://doi.org/10.1016/S0168-9002(01)00089-4
[23] T. Sjöstrand, S. Mrenna, P. Skands, A brief introduction to PYTHIA 8.1, Comput. Phys. Commun. 178 (2008) 852–867. arXiv:0710.3820, https://doi.org/10.1016/j.cpc.2008.01.036
[24] ATLAS Collaboration, The Pythia 8 A3 tune description of ATLAS minimum bias and inelastic measurements incorporating the Donnachie–Landshoff diffractive model, ATL-PHYS-PUB-2016-017, 2016. https://cds.cern.ch/record/2206965.
[25] ATLAS Collaboration, The ATLAS simulation infrastructure, Eur. Phys. J. C 70 (2010) 823. arXiv:1005.4568, https://doi.org/10.1140/epjc/s10052-010-1429-9
[26] S. Agostinelli, et al., GEANT4 – a simulation toolkit, Nucl. Instrum. Meth. A 506 (2003) 250. https://doi.org/10.1016/S0168-9002(03)01368-8
[27] ATLAS Collaboration, Performance of electron and photon triggers in ATLAS during LHC Run 2, Eur. Phys. J. C 80 (2020) 47. arXiv:1909.00761, https://doi.org/10.1140/epjc/s10052-019-7500-2
[28] ATLAS Collaboration, Configuration and performance of the ATLAS b-jet triggers in Run 2, Eur. Phys. J. C 81 (2021) 1087. arXiv:2106.03584, https://doi.org/10.1140/epjc/s10052-021-09775-5
[29] ATLAS Collaboration, ATLAS data quality operations and performance for 2015–2018 data-taking, JINST 15 (2020) P04003. arXiv:1911.04632, https://doi.org/10.1088/1748-0221/15/04/P04003
[30] ATLAS Collaboration, Vertex Reconstruction Performance of the ATLAS Detector at $\sqrt{s} = 13$ TeV, ATL-PHYS-PUB-2015-026, 2015. https://cds.cern.ch/record/2037717.
[31] M. Cacciari, G.P. Salam, G. Soyez, The anti-k_t jet clustering algorithm, JHEP 04 (2008) 063. arXiv:0802.1189, https://doi.org/10.1088/1126-6708/2008/04/063
[32] M. Cacciari, G.P. Salam, G. Soyez, FastJet user manual, Eur. Phys. J. C 72 (2012) 1896. arXiv:1111.6097, https://doi.org/10.1140/epjc/s10052-012-1896-2
[33] ATLAS Collaboration, Jet reconstruction and performance using particle flow with the ATLAS Detector, Eur. Phys. J. C 77 (2017) 466. arXiv:1703.10485, https://doi.org/10.1140/epjc/s10052-017-5031-2
[34] ATLAS Collaboration, Performance of pile-up mitigation techniques for jets in pp collisions at $\sqrt{s} = 8$ TeV using the ATLAS detector, Eur. Phys. J. C 76 (2016) 581. arXiv:1510.03823, https://doi.org/10.1140/epjc/s10052-016-4395-z
[35] ATLAS Collaboration, Forward jet vertex tagging using the particle flow algorithm, ATL-PHYS-PUB-2019-026, 2019. https://cds.cern.ch/record/2683100.
[36] ATLAS Collaboration, ATLAS flavour-tagging algorithms for the LHC Run 2 pp collision dataset, Eur. Phys. J. C 83 (2023) 681. arXiv:2211.16345, https://doi.org/10.1140/epjc/s10052-023-11699-1
[37] ATLAS Collaboration, ATLAS b-jet identification performance and efficiency measurement with $t\bar{t}$ events in pp collisions at $\sqrt{s} = 13$ TeV, Eur. Phys. J. C 79 (2019) 970. arXiv:1907.05120, https://doi.org/10.1140/epjc/s10052-019-7450-8
[38] ATLAS Collaboration, Measurement of the c-jet mistagging efficiency in $t\bar{t}$ events using pp collision data at $\sqrt{s} = 13$ TeV collected with the ATLAS detector, Eur. Phys. J. C 82 (2022) 95. arXiv:2109.10627, https://doi.org/10.1140/epjc/s10052-021-09843-w
[39] ATLAS Collaboration, Calibration of the light-flavour jet mistagging efficiency of the b-tagging algorithms with Z + jets events using $139\ \text{fb}^{-1}$ of ATLAS proton–proton collision data at $\sqrt{s} = 13$ TeV, Eur. Phys. J. C 83 (2023) 728. arXiv:2301.06319, https://doi.org/10.1140/epjc/s10052-023-11736-z
[40] ATLAS Collaboration, Flavor Tagging Efficiency Parametrisations with Graph Neural Networks, ATL-PHYS-PUB-2022-041, 2022. https://cds.cern.ch/record/2825433.
[41] ATLAS Collaboration, New techniques for jet calibration with the ATLAS detector, Eur. Phys. J. C 83 (2023) 761. arXiv:2303.17312, https://doi.org/10.1140/epjc/s10052-023-11837-9
[42] ATLAS Collaboration, Electron and photon performance measurements with the ATLAS detector using the 2015–2017 LHC proton–proton collision data, JINST 14 (2019) P12006. arXiv:1908.00005, https://doi.org/10.1088/1748-0221/14/12/P12006
[43] ATLAS Collaboration, Muon reconstruction performance of the ATLAS detector in proton–proton collision data at $\sqrt{s} = 13$ TeV, Eur. Phys. J. C 76 (2016) 292. arXiv:1603.05598, https://doi.org/10.1140/epjc/s10052-016-4120-y
[44] F. Chollet, et al., Keras, 2015. https://keras.io.
[45] M. Abadi, A. Agarwal, P. Barham, E. Brevdo, Z. Chen, C. Citro, G.S. Corrado, A. Davis, J. Dean, M. Devin, S. Ghemawat, I. Goodfellow, A. Harp, G. Irving, M. Isard, Y. Jia, R. Jozefowicz, L. Kaiser, M. Kudlur, J. Levenberg, D. Mané, R. Monga, S. Moore, D. Murray, C. Olah, M. Schuster, J. Shlens, B. Steiner, I. Sutskever, K. Talwar, P. Tucker, V. Vanhoucke, V. Vasudevan, F. Viégas, O. Vinyals, P. Warden, M. Wattenberg, M. Wicke, Y. Yu, X. Zheng, TensorFlow: Large-Scale Machine Learning on Heterogeneous Systems, 2015. Software available from tensorflow.org, https://www.tensorflow.org/.
[46] A.D. Martin, W.J. Stirling, R.S. Thorne, G. Watt, Uncertainties on α_S in global PDF analyses and implications for predicted hadronic cross sections, Eur. Phys. J. C 64 (2009) 653–680. arXiv:0905.3531, https://doi.org/10.1140/epjc/s10052-009-1164-2
[47] ATLAS Collaboration, Observation of electroweak production of two jets in association with an isolated photon and missing transverse momentum, and search for a Higgs boson decaying into invisible particles at 13 TeV with the ATLAS detector, Eur. Phys. J. C 82 (2022) 105. arXiv:2109.00925, https://doi.org/10.1140/epjc/s10052-021-09878-z
[48] M. Botje, J. Butterworth, A. Cooper-Sarkar, A. de Roeck, J. Feltesse, S. Forte, A. Glazov, J. Huston, R. McNulty, T. Sjostrand, R. Thorne, The PDF4LHC working group interim recommendations, 2011. arXiv:1101.0538
[49] ATLAS Collaboration, Luminosity determination in pp collisions at $\sqrt{s} = 13$ TeV using the ATLAS detector at the LHC, Eur. Phys. J. C 83 (2023) 982. arXiv:2212.09379, https://doi.org/10.1140/epjc/s10052-023-11747-w
[50] ATLAS Collaboration, Jet energy scale and resolution measured in proton–proton collisions at $\sqrt{s} = 13$ TeV with the ATLAS detector, Eur. Phys. J. C 81 (2021) 689. arXiv:2007.02645, https://doi.org/10.1140/epjc/s10052-021-09402-3
[51] K. Cranmer, G. Lewis, L. Moneta, A. Shibata, W. Verkerke, ROOT, HistFactory: a tool for creating statistical models for use with RooFit and RooStats (2012). https://cds.cern.ch/record/1456844, https://doi.org/10.17181/CERN-OPEN-2012-016
[52] W. Verkerke, D. Kirkby, The RooFit toolkit for data modeling, 2003. arXiv:physics/0306116
[53] W.A. Rolke, A.M. López, J. Conrad, Limits and confidence intervals in the presence of nuisance parameters, Nucl. Instrum. Meth. A 551 (2005) 493–503. arXiv:physics/0403059, https://doi.org/10.1016/j.nima.2005.05.068
[54] ATLAS Collaboration, ATLAS Computing Acknowledgements, ATL-SOFT-PUB-2025-001, 2025. https://cds.cern.ch/record/2922210.